

UC Irvine

UC Irvine Electronic Theses and Dissertations

Title

Fabrication of Nanotopographic Ophthalmic Device

Permalink

<https://escholarship.org/uc/item/40d852gj>

Author

Cai, Junming

Publication Date

2019

Copyright Information

This work is made available under the terms of a Creative Commons Attribution-NonCommercial-NoDerivatives License, available at <https://creativecommons.org/licenses/by-nc-nd/4.0/>

Peer reviewed|Thesis/dissertation

UNIVERSITY OF CALIFORNIA,
IRVINE

Fabrication of Nanotopographic Ophthalmic Device

Thesis

submitted in partial satisfaction of the requirements
for the degree of

MASTER OF SCIENCE

in Biomedical Engineering

by

Junming Cai (Jimmy)

Dissertation Committee:
Professor Albert F. Yee, Chair
Professor Eric Pearlman
Assistant Professor Wendy Liu

2019

DEDICATION

I dedicate this thesis to my parents, Jiangmei Lin and Zhiqiang Cai, for their immense support and patience to raise me to the person I am today. I also dedicate this thesis to my grandparents, to whom I owed eternal gratitude.

I would like to dedicate this to my long-time advisor and mentor, Prof. Albert F. Yee, for his inspiring guidance, model work ethics and forgiveness to my naivetes. I would also like to dedicate this thesis to late Dr. Roger Steinert who makes the artificial cornea work possible, to Dr. Marjan Farid, who makes all the clinical experiences possible with her world-class surgeon statute.

I dedicate this to the men and women in the LGBTQ+ community and their allies, for without their understanding, support and hard fight for equal rights, the world I live among will not be as bright as I discover.

Table of Contents

LIST OF FIGURES.....	iii
LIST OF TABLES	iv
ACKNOWLEDGMENTS.....	v
CURRICULUM VITAE	vii
ABSTRACT OF THE DISSERTATION.....	viii
Chapter 1. Introduction	1
1.1 Cornea Anatomy and Function.....	1
1.2 Biomechanical and Optical Property of the Cornea	2
1.3 Corneal Conditions Affecting Patient’s Visions	3
1.4 Overview of Treatment Options.....	3
1.5 Unmet Need of Tissue Based Replacement	4
1.6 A Brief Economic and Societal Case for Corneal Diseases Treatment	5
1.7 Status Quo: Medical Devices that interface with cornea	6
a. Boston Keratoprothesis.....	6
b. Contact Lens.....	7
Chapter 2: Improving Fabrication of Artificial Cornea Device	9
2.1 Artificial Cornea Design.....	9
2.2 Advantages of nanotopography	10
2.3 Fabrication advancement.....	11
2.4 Nanopatterning Advancement	11
2.3.1 Reversal Imprinting for nanotopography onlaying	11
2.4.2 r-NIL’s Theoretical limits and practical compromises	13
2.4.3 Polyurethane Elastomer Mold for Adaptive NIL	13
2.5 Material System Advances: PU.....	15
Chapter 3: In-vivo Study of Artificial Cornea Implant.....	16
3.1 Motivation.....	16
3.2 Method and Materials	16
3.2.1 Surgery and post-op care:.....	16
3.2.2 Method of Analysis:	17
3.3 Results & Discussion:	19
3.4 Crucial Lessons & Future Directions	21
Chapter 4: Fabrication of contact lens for antifungal property with nanotopography	22
4.1 Motivation.....	22

4.2 Proposed Nanopattern lens fabrication material system: PU/Chitosan	22
4.3 Crosslinking Strategy for Chitosan.....	24
4.3.1 Additive Crosslinking as molding strategy: TPP and Glutaldehyde with chitosan	24
4.3.2 UV-Crosslinkable N-MAC is a suitable candidate for a bandage contact lens prototype	24
4.4 Conclusion:	32
<i>Chapter 5 Mouse and Rabbit model for antifungal efficacy test.....</i>	32
5.1 Motivation.....	32
5.2 Murine Model Contact Lens Fabrication Protocol.....	33
5.3 Lens In Vivo Fitting Results.....	35
5.4 Further Work	35
5.5 Potential vessel for constructing a Fungal Infection Induction Model	36
<i>Chapter 6: Vacuum Assembly for Tunable Lens Fabrication.....</i>	37
6.1 Motivation.....	37
6.2 Materials and Method	37
6.3 Parts and Expose-Cut Assembly	39
6.4 Generic Protocol for Lens Prototyping with Vacuum Assembly	39
Part 1: Fabrication of PU nanopattern mold.....	39
Part 2: Assembly in vacuum mold.....	39
<i>Chapter 7: Commercialization Exploration of Artificial Cornea and Contact Lens.....</i>	40
7.1 I-CORP Experimental Iteration	40
7.1.1 Motivation	40
7.1.2 Research Method.....	40
7.1.3 Results.....	41
7.1.4 Discussion and Future Work	42
7.2 New Venture Competition (NVC)	42
<i>Chapter 8. Future Outlooks.....</i>	44
<i>References.....</i>	46

LIST OF FIGURES

FIGURE 1.1. ANATOMY OF A HUMAN EYE (TOP) AND CELLULAR HIERARCHY OF CORNEA (BOTTOM) ²	2
FIGURE 1.2. BRIEF PROCEDURE ILLUSTRATION OF KERATOPLASTY ⁷	4
FIGURE 1.3. GLOBAL TREND AND PREDICTIONS OF NUMBERS OF PEOPLE WHO ARE BLIND OR MODERATELY AND SEVERELY VISION IMPAIRED FROM 1990-2050 ¹⁰	6
FIGURE 1.4 SCHEMATICS OF THE ASSEMBLY OF THE BOSTON K-PRO (LEFT) AND IMPLANTED BOSTON K-PRO IN PATIENT (RIGHT)	6
FIGURE 2.1 SOLIDWORKS RENDERINGS OF FINAL DEVICE DESIGN. DIAMETERS AND THICKNESSES OF CENTRAL OPTIC ZONE AND SKIRT ARE INDICATED, AS ARE DIAMETER AND PLACEMENT OF SUTURE HOLES. ¹⁵	9
FIGURE 2.2 ADAPTED REVERSAL NANOIMPRINT LITHOGRAPHY (R-NIL) SCHEME AND SAMPLE HOLDING DEVICES. (A) SCHEME OF ADAPTED R-NIL FOR APPLICATION OF PMMA PILLARS TO A CURVED PMMA SURFACE. (B) CUT-AWAY RENDERING OF SOLIDWORKS MODEL OF THE HOLDER DEVICE ADAPTED FOR ALIGNING THE LENS, CURVING THE PDMS ELASTOMER MOLD, AND TRANSFERRING THE FORCE FROM THE PLANAR TOP AND BOTTOM PLATES TO THE CURVED SURFACES (C) PHOTOGRAPH OF THE CUSTOM-BUILT HOLDER ASSEMBLY. ²¹	12
FIGURE 2.3 IMPLEMENTATION SCHEMATICS OF ADAPTIVE NIL WITH POLYURETHANE	14
FIGURE 2.4 NANOPATTERNED PMMA-BASED LENS WITH ADAPTIVE NIL (LEFT), AND SEM IMAGE OF THE NANOPATTERN TRANSFERRED ON THE LENS SURFACE (RIGHT)	15
FIGURE 3.1 WORKFLOW SCHEMATICS OF THE PILOT ANIMAL IMPLANTATION	17
FIGURE 3.2 SLIT LAMP (TOP) AND AS-OCT (BOTTOM) OF THE IMPLANTED RABBIT EYE BEFORE AND AFTER ONE MONTH PERIOD	20
FIGURE 3.3 SCANNING ELECTRON MICROGRAPHS INDICATES NANOPATTERNS RETAIN HIGH FIDELITY AFTER ONE-MONTH IMPLANT	21
FIGURE 4.1 SEM OF ASSORTED CHITOSAN-BASED NANOPATTERN AND PMMA REPLICA AS QUALITY CONTROL	23
FIGURE 4.2 N-MAC SYNTHESIS MECHANISM: THE FUNCTIONAL AMINE GROUP ON THE DEACYLATED CHITOSAN IS ATTACHED BY ONE BRANCH OF THE METHACRYLATE ANHYDRIDE. THE ADDITIONAL SUBSTITUENT CARRIES THE DOUBLE BOND REQUIRED TO BE UV-ACTIVATED ON DEMAND BY RADICALLY EXCITED INITIATORS. ²⁶	25
FIGURE 4.3 SYNTHETIC WORKFLOW SCHEMATICS OF N-MAC	26
FIGURE 4.4 FTIR SPECTRUM OF N-MAC SHOWING THE ADDITION AND ALTERATION OF AMINE GROUP AND DOUBLE BONDS	27
FIGURE 4.5 CONSISTENT SWELLING AND DRYING BEHAVIOR OF N-MAC UNDER VARIOUS CROSSLINKING EXPOSURE TIME	29
FIGURE 4.6 UV-VIS ABSORPTION SPECTRUM OF THE CROSSLINKED N-MAC SHOWS MINIMAL ABSORPTION OF VISIBLE LIGHTS	30
FIGURE 4.7 NANOPATTERNED N-MAC GEL SURFACE HAS GOOD FIDELITY OF THE REVERSE REPLICATION	31
FIGURE 5.1 REPRESENTATIVE IMAGES OF A MURINE CORNEA AFTER WEARING A P. AERUGINOSA-INOCULATED CL FOR 22 DAYS WITHOUT THE DEVELOPMENT OF BACTERIAL KERATITIS. DISSECTING MICROSCOPE IMAGE (LEFT) AND CONFOCAL IMAGE (RIGHT) ¹⁸	33
FIGURE 5.2 FABRICATION OF MURINE LENS MOLD AND MOLDING MOUSE LENS WITH TWO CHITOSAN-BASED HYDROGELS	34
FIGURE 5.3 MURINE LENS OF N-MAC UNDER STEREOMICROSCOPE, BOTTOM-UP VIEW (LEFT) AND SIDE VIEW (RIGHT)	34
FIGURE 5.4 MURINE LENS OF CHITOSAN-TPP FITTED UNDER MICROSCOPE, INITIAL TIME POINT VIEW (TOP) AND AFTER ONE DAY (RIGHT)	35
FIGURE 5.5 ILLUSTRATION TO APPLY FUNGAL INFECTION INDUCTION MODEL	36
FIGURE 6.1 MECHANISTIC ILLUSTRATION OF VACUUM LENS FABRICATION ASSEMBLY	37
FIGURE 6.2 SOLIDWORKS RENDERING OF VACUUM LENS FABRICATION ASSEMBLY (LEFT: BY PARTS; RIGHT: BY CLOSED ASSEMBLY)	39
FIGURE 7.1. SCHEMATICS OF REVENUE STREAMS IN THE PROPOSED LICENSING BUSINESS MODEL FOR GLOBAL EXPANSION.	43

FIGURE 7.2 TOTAL AVAILABLE MARKET (TAM, IN LARGE CIRCLES) AND SERVICEABLE OBTAINABLE MARKET (SOM, IN RAINDROPS) OF POTENTIAL REGIONS AROUND THE GLOBE. PROJECTED BUSINESS ADVANCEMENT TIMELINE IS ALSO LISTED BELOW IN MAPS. WITH LICENSING MODEL, THE COMBINE OF BOTH PRODUCT LINE INTERNATIONALLY COULD GENERATE AN ESTIMATE REVENUE OF \$16.4 M. CREDIT: WYOBROSKI AND CAI 44

LIST OF TABLES

TABLE 1: REFLECTIVE INDEX OF USED MATERIALS	2
TABLE 2: VALUE PROPOSITION PROGRESSION	41
TABLE 3: TARGET CUSTOMERS	41

ACKNOWLEDGMENTS

I sincerely thank my advisor, Professor Albert F. Yee for his support, understanding and intelligent inspirations. As in Chinese culture, we acknowledge mentors as fathers. I have been honored to have his fatherly nourishment both academically and personally, despite my ups and downs in life. I'm also grateful for the advice from my other committee members: Prof. Eric Pearlman and Prof. Wendy Liu, who advice and support my research and academic growth directly.

I also have great gratitude to my wide list of collaborators, Prof. Szu-Wen Wang, Dr. Marjan Farid, Dr. Kate Xie, Dr. Priscilla Vu, Dr. Steven Carters, Prof. Catherine Loudon, for without their board and comprehensive expertise and resources, this thesis would not be as substantial.

I also am thankful for all the previous and current Yee's lab members' help throughout my years in UCI. I thank my previous undergraduate mentors Dr. Mary Dickson and Dr. Elena Liang, who jumpstart the artificial cornea project as well as my research career. My fellow graudate lab members: Xin Fu, Sara Heedy, Rachel Rosenweig, Yasaman Fatapour, Rebecca Wybroski, Ming Yang, Yuhang Cai, and Jerry Lin, for their day-to-day practical tips and companionship along the graduate school life. I also thank all the undergraduates mentees: Sydney Tea, Andon Spassov, Jingyi Luo, Alex Parviar and BME BioEngine team of 2018 and 2019, that believe and team up with me to make all the work here possible.

I would also like to thank all the staff and faculty that provide technical and administrative support for my work to smoothly progress. From BME department, Clare Cheng, and Maggie Mulcare and from CBE department, Elizabeth Randall, Yi-San Chang-Yen, Steve Weistock. External Support from Dr. Paul Blaze and Victor Sazo from Optimax for artificial cornea manufacturing.

Finally, I would like to thank my funding source: UCI UROP, New Venture Competition, Congressionally Direct Medical Research Program (CDMRP), NSF I-CORP and Applied Innovation. Thanks for their generous financial support to make all the research into reality.

CURRICULUM VITAE

Junming Cai (Jimmy)

- 2017 B.S. in Biomedical Engineering, University of California, Irvine
 B.S. in Material Science Engineering, University of California, Irvine
- 2019 M.S. in Biomedical Engineering, University of California, Irvine

FIELD OF STUDY

Biomedical Engineering, Biomaterials, Nanofabrication, Clinical Study

PRESENTATIONS

1. **Cai J**, Farid M, Yee AF. A Novel Synthetic Artificial Cornea with Biomimetic Nanotopography, from Device Fabrication to Animal Study.
Oral presentation at UC Systemwide Bioengineering Symposium, June 2018, Riverside, CA.
Poster Presentation at BMES, October 2018, Atlanta, GA
2. Xie K, Liang E, **Cai J**, Vu P, Carter S, Yee AF and Farid M, In Quest of a Novel Artificial Cornea Using Biomimetic Nanotopography: Biocompatibility Studies in the New Zealand White Rabbit.
Poster Presentation at ASCRS, April 2018, Honolulu, Hawaii

ABSTRACT OF THE DISSERTATION

Fabrication of Nanotopographic Ophthalmic Device

By Junming Cai (Jimmy)

Master of Science in Biomedical Engineering

University of California, Irvine, 2019

Professor Albert F. Yee, Chair

Corneal disease is the second most prevalent cause of blindness in the world.

Keratoplasty or corneal transplant is available as the last treatment resort and extended drug delivery following the procedure are preferred to be delivered by a drug eluting contact lens. Patients using either device in the wounded eye are prone to microbial infection that could complicate the outcome of the sight recovery. Thus, nanotopography, a physical surface modification studied to have potential antimicrobial effect and wound healing promotion, is considered to be integrated in novel design of both devices. Due to the spherical nature of the eye, conventional nanotechnology could not produce such surface, or requires heavy cost and resources.

In this thesis, I : 1) improve a nanopatterning technique for spherical surface and apply it on a novel cornea device, 2) validate its biological responses in vivo, 3) apply the patterning technique for a contact lens design with a new class of material, 4) analyze the economic and commercial benefits of both device in current ophthalmic market. This thesis consists universal protocol for adaptive patterning methods on various material platform and outline validation method for future regulatory works. This thesis shall set the foundation for a medical device startups that could restore sights for millions around the world.

Chapter 1. Introduction

1.1 Cornea Anatomy and Function

Eye is an essential organ in human's sensory system. Estimated approximately 80% of our perceived information comes from vision. Eye is also a highly complex and intricate system. The major structures of the eye are illustrated. The wall of the eye consists of three concentric layers: an outer layer, a middle layer, and an inner layer. The outer layer, which is fibrous, includes the cornea, corneal epithelium, conjunctiva, and sclera. The middle layer, which is vascular, includes the iris and the choroid. The inner layer, which is neural, contains the retina.¹ Healthy eye provides a precise and agile control of focal system that transmit and transduce light signals to our central nervous system.

Cornea, the clear, dome-shaped front portion of the eye, is responsible to focus light from the environment onto the back side of the eye where retina converts light signals into neural signals for perception formation. The cornea is comprised of five layers: the outermost corneal epithelium, which consists of superficial epithelial cells, central superbasal epithelial cells and an inner single layer of basal epithelial cells; the Bowman's layer; the corneal stroma which is populated by keratocytes; the Descemet's membrane and the inner corneal endothelium, which is a monolayer of neural crest-derived endothelial cells.²

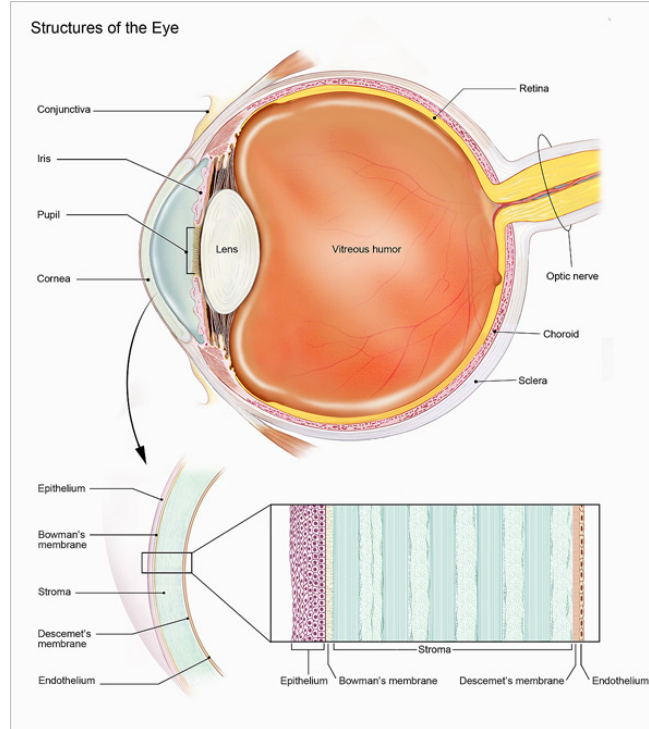


Figure 1.1. Anatomy of a Human Eye (top) and Cellular Hierarchy of Cornea (bottom)²

1.2 Biomechanical and Optical Property of the Cornea

Cornea's laminar layering provides high optical transparency and anisotropic elastic property. Due to orderly arrangement of collagen fibrils in the cornea, it is highly transparent with transmission above 95% in the spectral range of 400-900 nm. The refractive index of the cornea is $n \approx 1.3765 \pm 0.0005$. The remaining components between cornea and the retina has a range of refractive index from 1.335 to 1.42.³ However, regeneration of the cornea from heavy trauma is short of enough guidance. The less organized scarring process usually lead to blurry vision and would worsen overtime due to the abnormality in its mechanical performance.⁴

Table 1: Reflective index of used materials

Material	PMMA	Polyurethane (Texin)	Chitosan
Refractive Index (n)	1.481-1.499	1.51 ⁵	1.332-1.336 ⁶

1.3 Corneal Conditions Affecting Patient's Visions

The cornea could be affected by a wide range of conditions that could lead to visual impairment. The external source of the conditions could be physical, chemical or biological. Physical injury is induced by foreign objects with abrupt forces that scratches or even penetrates into the eye. Corrosive chemicals exposure, such as strong acid and base splash, is a primary example of chemical source. Also, commonly, pathogens including bacteria, viruses, fungi and parasites, could infect corneal tissue and cause inflammatory condition medically called keratitis.

² Another major class of conditions that affect patient's visual is corneal dystrophies.

Keratoconus and Fuch's Dystrophy are two of the more common types within the class. Unlike the previous mentioned, corneal dystrophies are usually inherited through family history, and generally progress relatively slowly. Thus, they tend to be mostly diagnosed in professional settings.

1.4 Overview of Treatment Options

Treatments to recover vision for cornea related diseases are available, and have developed progressively in recent years, thanks to various technological advancements including the integrative use of laser in ophthalmology. Phototherapeutic keratectomy (PTK) is the technique that utilize laser or UV light source to reform the cornea into a healthier stage, and usually applied to delay the need of more invasive procedures. In severe cases, however, surgical corneal grafting or corneal replacement is required to restore better visual outcome. Corneal transplant, medically termed keratoplasty, is the more invasive group of options to rescue patient's eyesight. It is typically performed under anesthesia and outpatient in designated eye centers or ophthalmic clinics. A portion of or the whole cornea is removed and replaced by an external healthy counterpart, and anchored by surgical sutures by trained ophthalmologists, shown in the illustration below. (Figure 1.2) Based on the replacement, keratoplasty could be

further sectioned into partial thickness transplant consisting of anterior lamellar keratoplasty, endothelial lamellar keratoplasty, and full thickness transplant or penetrating keratoplasty.

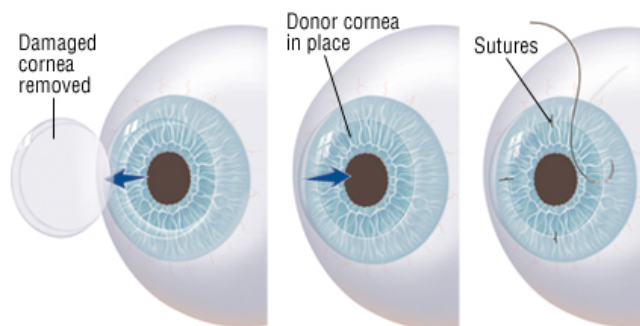


*Figure 1.2. Brief Procedure Illustration of Keratoplasty*⁷

Performing keratoplasty relies on not only skilled surgeons, but also sourcing visually functional cornea tissue or corneal device. Corneas, as the most transplanted tissue worldwide, are consumed more than 47,000 times in the United States alone in 2014. The majority of these transplants uses donor tissues, with a small fraction (~1%) taken by artificial cornea replacement.

1.5 Unmet Need of Tissue Based Replacement

Nearly five million people in the world are affected by corneal blindness, which affects the front part of the eye crucial for light passage and clear vision. Current treatment options are limited to donor corneas and early artificial devices such as the Boston Keratoprosthesis (KPro). Of the 12.7 million people around the world waitlisted for donor this life-changing treatment, only 400 patients will receive artificial corneas and 185,000 will receive donor corneas each year. The 1-2% of patients who regain their sight through currently available prosthetic and donor corneas experience high complication rates. Donor corneas have a ten-year rejection rate of approximately 40%, and the KPro device has been recorded to have bacterial infection rates as high as 13%.⁸ These numbers are currently mitigated by a lifetime regimen of daily

antimicrobial eyedrops and immune-suppressive prescriptions; however, such measures fail to alleviate the risks for noncompliant patients. Despite medical procedures exist to reverse poor vision for patients in need, contrasting gap of global demand and supply of such tissue replacement is urgently calling for innovation.

1.6 A Brief Economic and Societal Case for Corneal Diseases Treatment

Optimal vision impacts directly on every stage of human development as well as social productivity. A CDC study estimated that the United States' expenditure on major visual disorders of \$35.4 billion comprised of \$16.2 billion in direct medical costs, \$11.1 billion in other direct costs, and \$8 billion in productivity losses, in 2004. Annually, the federal government and state Medicaid agencies pay at least \$13.7 billion of these costs.⁹

Besides the immediate and direct constraining effect on the economics, visual disease epidemics could further toll the patients and the society beyond the medical bills. Blindness, the loss of vision, one of the most devastating deuteriations of vision, impacts estimated 36 million people worldwide and projected to impact more than 100 million people by 2050. It accompanied by current 200 million cases of moderately or severely vision impaired with the predicted population exploding into 600 million by 2050.¹⁰ In the EU alone, for example, these conditions result in the combined loss of productivity priced from €25.83-56.52 billion annually.¹¹

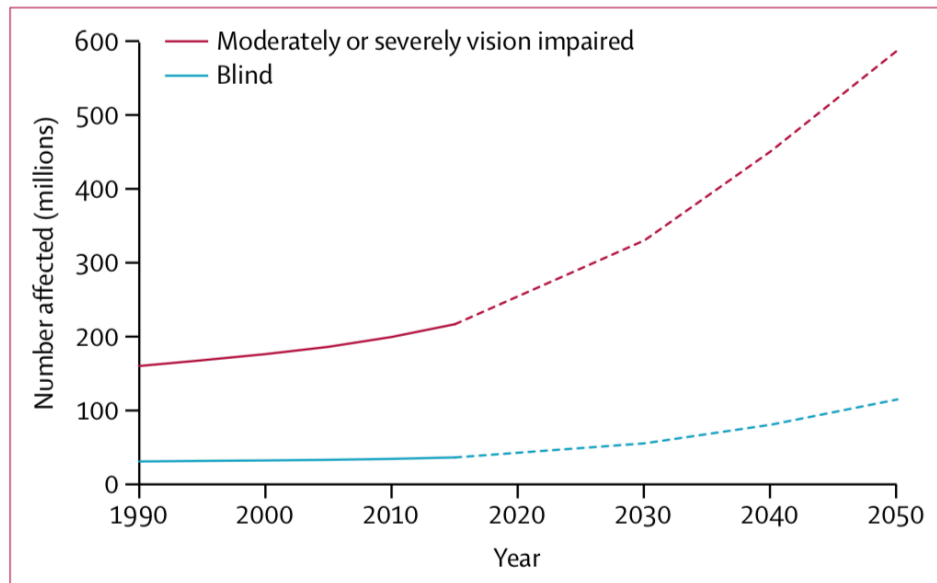


Figure 1.3. Global Trend and Predictions of Numbers of People Who Are Blind or Moderately and Severely Vision Impaired from 1990-2050¹⁰

1.7 Status Quo: Medical Devices that interface with cornea

a. Boston Keratoprosthesis

The current Boston Keraoprosthesis could compose of a rigid PMMA front plate as the support of a donor corneal graft, a fenestrated titanium backing, titanium locking ring and a front plate locking stem. Together with harvested corneal tissue, the device is assembled on surgical table and sutured into patient's eye. (Fig. 1.4)

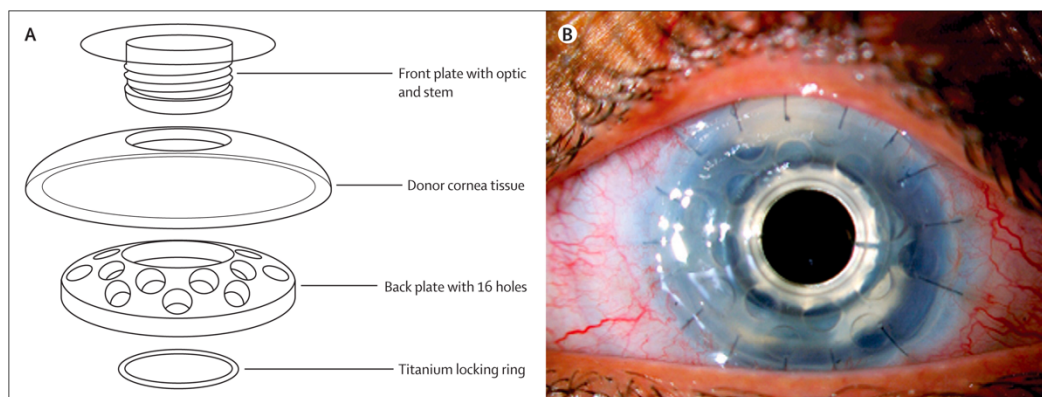


Figure 1.4 Schematics of the Assembly of the Boston K-Pro (Left) and Implanted Boston K-Pro in Patient (Right)

Indication and Complications:

Keratoprosthetics have been considered to be the last resort of surgical intervention for corneal-blind patients when ophthalmologist compounds the treatment decision factors including cost, visual outcome improvement and invasiveness. The current Boston KPro indication has primarily been patients with failed penetrative keratoprosthesis, aniridia, and acute ocular trauma such as chemical burns, herpes keratitis, corneal dystrophies, and Steven Johnson Syndrome.^{2,11} On top of diagnosis, dry eye syndromes would also impose limitation for deploying keratoprosthesis, because the lack of abundant tear film will constrain the device efficacy and post-op recovery. Such sub-optimal implant could lead to surrounding tissue melts, extrusion of device, endophthalmitis, and even the loss of operated eye.

The status quo Boston Keratoprosthesis sets some ground work in addressing the corneal replacement conditions. It has clinical track records from some of the implants functioning for more than 10 years inside a patient, proven that device's biocompatibility and mechanical durability has to be suitable for the dynamic environment of the eye. Optically, its transparency is comparable to natural healthy corneal tissue, when no complications occur.

However, regrettably, the Boston KPro only has these ideal outcomes when all odds are in favor to the patients. High variability of the visual acuity, lack of personal adaptability, sizable rejection rate stemming from its susceptibility to pathogens, are a few of the drawbacks of Boston KPro that demands new innovation to catch up and resolve. Only when those issues are mitigated will artificial corneal replacement become clinically, economically and societally favorable.

b. Contact Lens

Need for Contact Lens/Risk of microbial keratitis

Contact lens is an eyecare accessory medical device reside on top of the tear film above the cornea, which provide vision aids or other ophthalmic therapeutics, or occasionally for cosmetic purposes. It composes of a wide range of materials, primarily polymeric base. It could be categories generally into, soft hydrogel lens, hard contact lens, and gas permeable silicone lens. By replacement variation, it could be sorted into, daily, weekly and monthly disposables. By acquisition method, some could be purchased over the counter while some equipped with customized visual correction or therapeutic function will require prescriptions.²

Status Quo for Contact Lens

Contact lens is the second most popular medical devices in the United States, with 45 million users wearing them to correct sights, improving people's quality of life and productivity seamlessly.¹¹ With a large range of product selections for different purposes, and relatively superficial consumer education related their risks and proper caring habits, contact lens has looming risks of eye infections including microbial keratitis that could undercut their benefits.¹³ Infections induced by improper care could contribute to blindness at a startling rate of 1 out of 500 contact lens users, causing approximately 1 million hospital visits and directly costing the US healthcare system in estimate \$175 million annually.^{14,15} Even when contact lens related infections have not gotten as grave as blindness, the array of symptoms covering from redness and discomfort of the eye to involuntary tearing and discharge with blurry vision, still has severe consequences to patients-in-need.

What does contact lens demands?

New and existing products with additional layers of eyecare accessories have been introduced by companies to curtail the infection prospects. The user's awareness has also been

growing under the help of corporations, government agency and public health advocacies. Even so, contact lens are still plagued by the invasion of pathogens. Therefore, eradicating the breeding ground for the pathogens poses highly effective preventive value medically and economically. On top of lens' basic requirement to be optically transparent, mechanically durable under delicate handling, and high oxygen permeability to sustain cornea's health, a novel solution shall also concentrate on providing sustained preventative measures against infectious agents.

Chapter 2: Improving Fabrication of Artificial Cornea Device

In this chapter, we will introduce our first-generation cornea device, in its fabrication details, material, and design. It will be followed up by improvements on each of the three aforementioned segment and the realization of the second-generation cornea implant.

2.1 Artificial Cornea Design

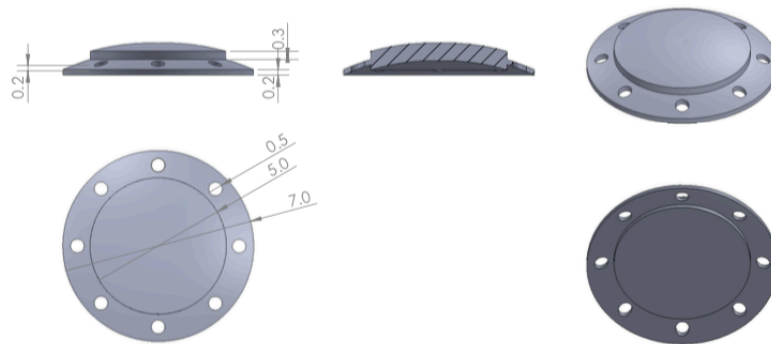


Figure 2.1 Solidworks renderings of final device design. Diameters and thicknesses of central optic zone and skirt are indicated, as are diameter and placement of suture holes.¹⁵

Previously, artificial cornea device is designed with a two-step spherical lens shape is decorated with suture holes on the periphery.¹⁶ The radius of curvature is set to be 780 mm, similar to human's average anatomical value.¹⁷ The protruded central optical region raises 0.3

mm above the peripheral surface. This elevation is intended to create a physical contact barrier to inhibit scarring tissue to overgrow onto the primary light path, giving the device better consistency on the recovered visual clarity after implantation. The skirt of the implant is designed to be 0.2 mm thick, to minimize the difficulty for the ophthalmologist to create a tissue pocket and to fit the device into the pocket. This could be beneficial for recovery because less incision could accelerate the healing timeline. The separation of the two spherical surfaces is setup to provide a platform to implement two different type of nanotopography, that could provide different biological effect to surrounding environment, in the fabrication process. The suture holes dimension is consistent with the suture diameters and adjusted to maximize the comfort of the surgeon's operation.

Some future flexibility on the design are envisioned to adopt further on manufacturability and functionality. First, radius of curvatures on the front and the back side could both vary to endorse optical power for patients in need of vision correction. Second, number of Suture holes could be increased if higher oxygen permeability is desired.

2.2 Advantages of nanotopography

Topography, the surface texture, of the material is one of the biophysical cues that could potentially influence its interfacing biological's cellular response. Nanopillar, inspired by natural insect wings' surface, has been studied for its antibacterial and antifungal property.¹⁷⁻¹⁹

Nanolines are more often observed to have an influence on mammalian cells guidance and alignment.²⁰ Matching nanopattern's functionality accordingly onto regions or segments in the tissue could achieve spatial control of the device neighboring surrounding and optimize the implant outcome. Using nanopatterns instead of other chemical or biological cues is advantages in several fronts. First, surface modification is passive and physical. Second, surface

modification is more sustainable than chemical cues that could be consumed or degraded in the long terms. Thirdly, Surface modification could induce desirable effect in a shorter and more precise range, preventing unwanted off-targeting effect in a global scale.

2.3 Fabrication advancement

Traditionally, similar to prescribed hard contact lens, the artificial cornea design is realized on initially PMMA using semi-automated CNC diamond-tip lathe. In brief, the design space is carried out in the 4 following steps: Step 1: carve out front and back curvature and polish down to thickness; Step 2: controlled frontal cut to accentuate central optics platform; Step 3: Optical polish to achieve clarity; Step 4: Fenestration or controlled drilling of suture holes

The primary reason to obey the described order to reduce materials to shape is with regards to potential skirt fracture during thinning. Power tool requires high shear stress on the skirt of the device during the thinning process and accompanied by the significant reduction of the material thickness, relatively brittle PMMA could fail in bulk through fracture instead. Thus, machining skirt with lathing has its reproducible limit down to 0.2 mm thick, although physicians prefer thinner (~150 micron) for easier insertion during procedure.

In the future, to further reduce cost, volume of production and reproducibility, injection molding would be more preferable for prototyping than semi-automated machining.

2.4 Nanopatterning Advancement

2.3.1 Reversal Imprinting for nanotopography onlaying

With the adaptation of previous work by Dickson et al., nanopatterns are transferred to the cornea lens. In brief, prepared and filtered 5 wt% medical grade Poly (methyl methacrylate) (PMMA) (>1MDa) toluene solution are spincoat cast on a PDMS nanomold replicated from a

nickel or silicon master, at 600 RPM for 45 seconds. The film is annealed on the hot plate at 100 °C for 1 hr.¹⁶

The nanostructure film is then pressed against the cornea lens in a 3-part assembly, under 3 MPa in the Tetrahedron pneumatic press, at 105 °C for 10 minutes and actively cooled down to room temperature for 10 minutes before detachment from the PDMS mold.

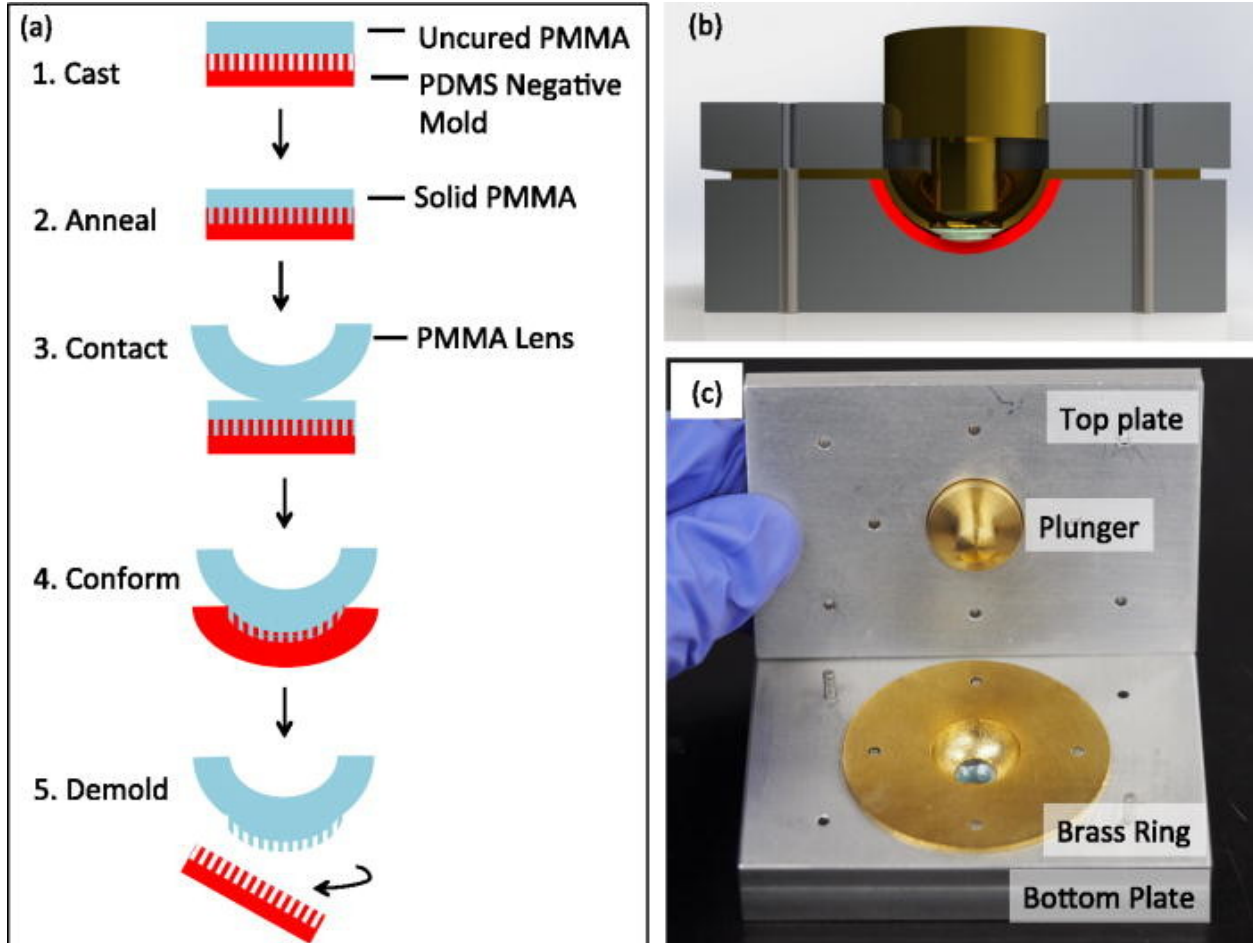


Figure 2.2 Adapted reversal nanoimprint lithography (r-NIL) scheme and sample holding devices. (a) Scheme of adapted r-NIL for application of PMMA pillars to a curved PMMA surface. (b) Cut-away rendering of solidworks model of the holder device adapted for aligning the lens, curving the PDMS elastomer mold, and transferring the force from the planar top and bottom plates to the curved surfaces (c) Photograph of the custom-built holder assembly.²¹

To accommodate the curved and complex geometry in the cornea device, an adaptive way to transfer nanotopography from 2D flat surface to 3D curvature is necessary. Reversal nanoimprint lithography is using the principle where polymer at glass transition temperature will

present more viscous behavior and material with the same transition temperature could flow into each other at the contact boundary and merge, where pre-patterned film could adhere and transfer onto the bulk lens design.

2.4.2 r-NIL's Theoretical limits and practical compromises

Although thin film could be conformal onto geometry, a two-dimensional surface mathematically could not perfectly fold onto a spherical surface without deformation. According to Gauss's Theorema Egregium in 17th century, a sphere of radius R has constant Gaussian curvature which is equal to $1/R^2$. At the same time, a plane has zero Gaussian curvature. As a corollary of Theorema Egregium, a piece of paper cannot be bent onto a sphere without crumpling. Conversely, the surface of a sphere cannot be unfolded onto a flat plane without distorting the distances. If one were to step on an empty egg shell, its edges have to split in expansion before being flattened. Mathematically, a sphere and a plane are not isometric, even locally. One significant application of this theorem is in cartography: it implies that no planar (flat) map of Earth can be perfect, even for a portion of the Earth's surface. Thus every cartographic projection necessarily distorts at least some distances.”²² Creases or concentrated stretching of the film could provide blind spot for pathogen to opportunistically reproduce and propagate. Furthermore, distortion above micron level could affect the optical appearance of the device, if landed at the optical path.

2.4.3 Polyurethane Elastomer Mold for Adaptive NIL

Adaptive NIL is an alternative nanopatterning method purposed for the curved ocular device fabrication. The principle is similar to NIL where patterns are pressed and formed under elevated temperature and pressure, enabling the polymeric substrate to flow and controllably deformed to acquire the mold's pattern. The novelty of this method is to use materials that is

capable of carrying nanopattern at high fidelity from a traditional flat planar master, made by either silicon or etched metal surfaces, and onlaying patterns onto spherical surface tightly with the mold's high tensile strain. Similar to a removable tattoo sticker, where tattoo artists comply and design patterns on flat paper but transfer them onto a thin sticker that wrap the customer's body part for templating.

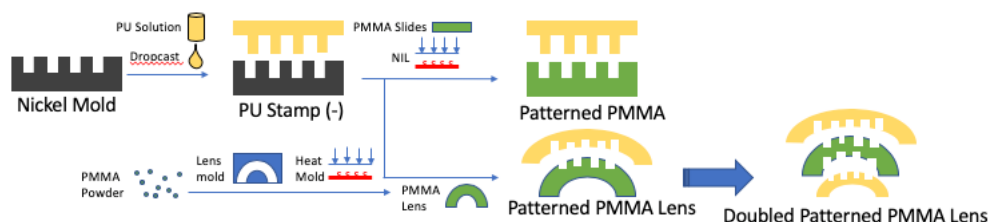


Figure 2.3 Implementation Schematics of Adaptive NIL with Polyurethane

10wt% PU in DMF Solution was prepared by measuring 1.5g PU particles and 13.5g DMF in fume hood and mixing in 20 mL scintillator vial. The mixture is gently heated between 70-80 °C for 2 days. The prepared solution is then dropcast on a master mold and annealed at 80 °C for a minimum of 30 minutes. The cast thin film mold is spray-coated with Teflon spray from Dupont and pressed directly on the cornea or contact lens designated patterning area, either single side or double sides, in the similar assembly used in reversal imprinting. The imprinting process will be under 3 MPa at 100 °C for 20 mins and actively cooled for another 10 minutes.

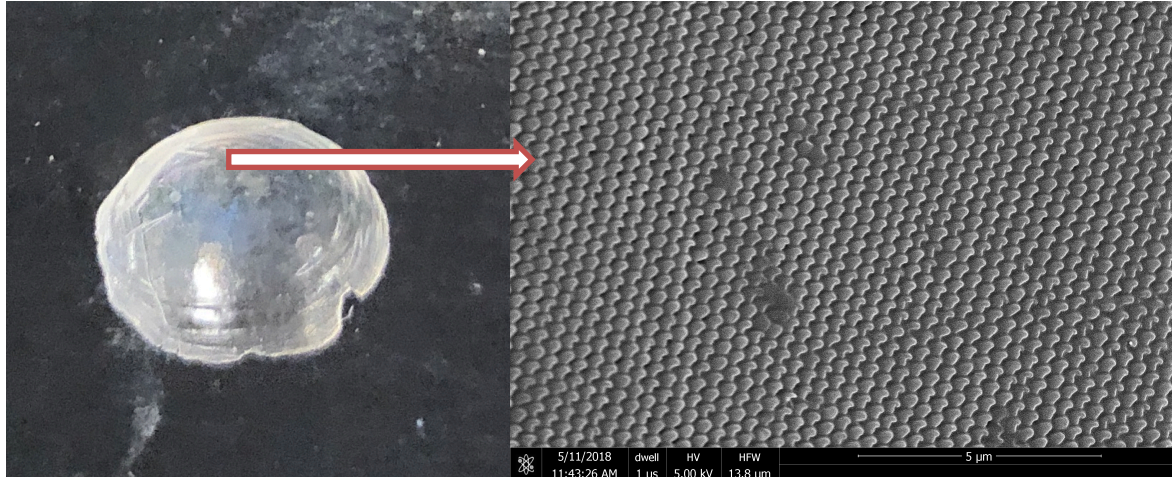


Figure 2.4 Nanopatterned PMMA-based lens with Adaptive NIL (left), and SEM image of the nanopattern transferred on the lens surface (Right)

2.5 Material System Advances: PU

Polymethylmethacrylate (PMMA) is a material class approved by FDA for ocular use, and previously adopted by Boston Keratoprothesis. It has high optical transparency, high young's modulus, intermediate glass transition temperature, and historically good biocompatibility in the ocular environment. However, it's relatively inflexible and brittle compare to other rubbery polymers, which impose extra caution for the surgeon for handling the device in operation.

Polyurethane is a widely used elastomer for commercial products. Selected variation has good elasticity, comparable transparency and intermediate glass transition temperature. Although it is not yet approved by the FDA specifically in ocular application, it's been historically applied in other medical environment such as vascular grafts.²³

We utilize the manufacturing advancement mentioned and adapt the craftsmanship onto PU instead. For it's less brittle and flexible, the prototype's skirt could be further reduced. The thin skirt additionally enables the elimination of pre-disposition of suture holes. As demonstrated on the left, the skirt is thin enough for the suture needle to puncture through. The removal of the fenestration step simplifies the manufacturing process.

Furthermore, as shown on the right, the surgeon could bend (or lively described as “taco-ing” technique) with tweezers. This potentially allows surgeons to create a smaller incision and applying less pressure for the device deploying, which makes the procedure less risky. The small wound could potentially heal faster, bettering patient’s experience after the surgery.

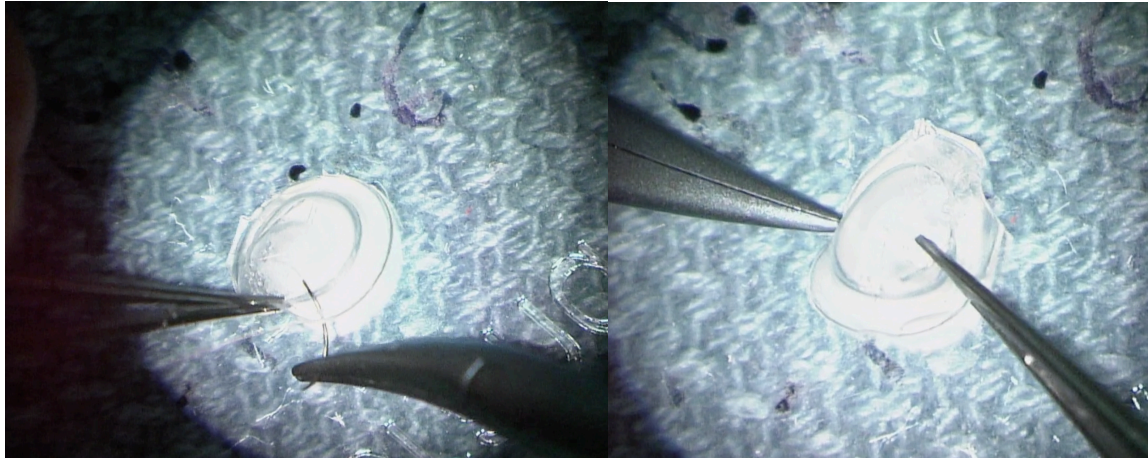


Figure 2.5 PU-based cornea prototype is tested for bending and suturing. Implantability and Easy Maneuver were more preferred by surgeon. Video Credit: Dr. Marjan Farid

Chapter 3: In-vivo Study of Artificial Cornea Implant

3.1 Motivation

From the previous chapter, artificial cornea could be prototyped in a laboratory setting as designed for *in-vivo* testing. Thus, in this chapter, a pilot study involving animal subjects are conducted, with the primary anticipation to observe the live animals’ response to the implants and the implants durability in practice. The study hopes to refine surgical and experimental protocols for a more populous cohort.

3.2 Method and Materials

3.2.1 Surgery and post-op care:

Two artificial cornea prototypes made from polymethylmethacrylate (PMMA) with a central antimicrobial nanotopography onlay were implanted into the right eyes of 2 New Zealand white rabbits. In one rabbit, a crescent blade was used to create a plane within the stroma to place

the skirt of the device. In the other, the femtosecond laser was used to create a plane within the stroma. Slit lamp and anterior segment optical coherence tomography photos were obtained twice a week for the first week, then weekly over a one-month period. During the period, topical or subconjunctival antibiotics are given to the subjects daily. The procedures are adopted from current surgical practice in clinics, consulted and modified with the expertise introduced by Dr. Farid and her associates, and approved by UC Irvine IUCAC committee.

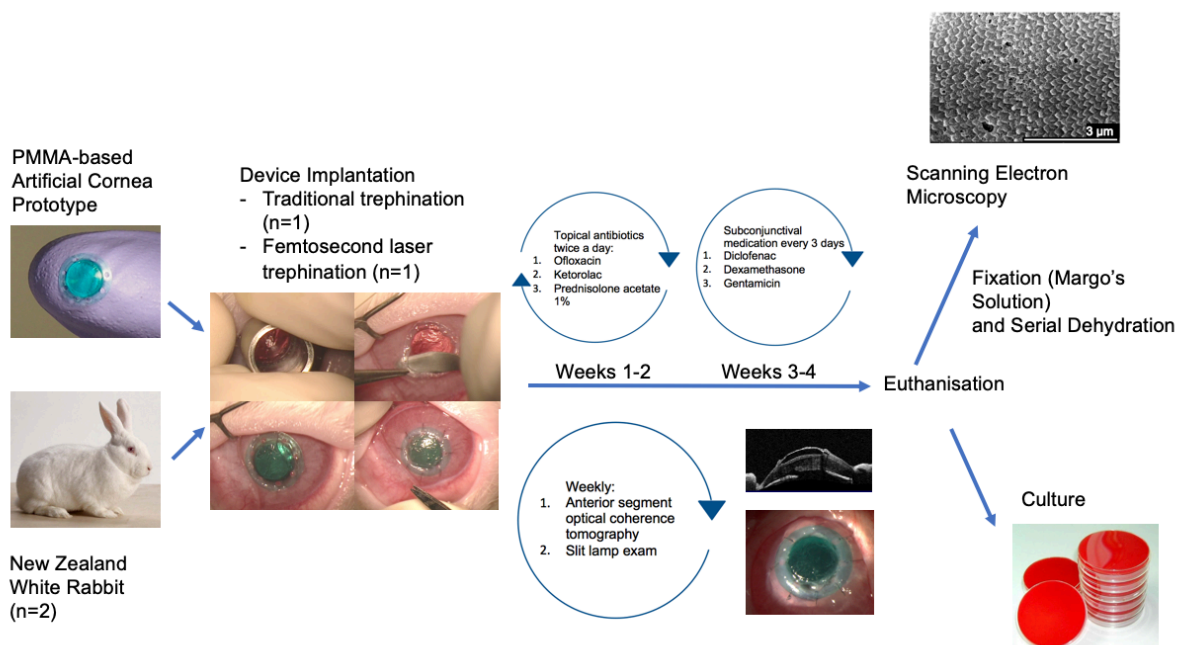


Figure 3.1 Workflow Schematics of the Pilot Animal Implantation

3.2.2 Method of Analysis:

a. Slit Lamp

A slit lamp is a bright field microscope with a bright light projected through a think slit used during an eye exam. It visualizes different structures at the front of the eye and inside the eye. Eye drop with fluorescein is applied during this portion of the exam to highlight the boundary between implant and cornea tissue.

b. AS-OCT

Anterior Segment Optical Coherence Tomography (AS-OCT) takes cross-sectional images of the cornea and anterior segment are produced with optical backscattering of light in a fashion analogous to B-scan ultrasonography. Because light travels much faster than sound, the time delay of the returning light reflection in OCT is determined indirectly by the method of low-coherence interferometry. Optical interferometry is used to determine the distance to reflective structures within the eye. The OCT uses a noncontact image acquisition method that is efficient and safe.

To measure the animal's cornea profile, a Visante OCT (Carl Zeiss Meditec, Dublin, CA) is operated by trained technician. The animal under general anesthesia is held up into the position where the eye is directly looking into the measurement window for several seconds. Both side profiles and cornea's height landscape could be obtained with integrated software in post processing.

c. Fixation and SEM

To fix the enucleated samples, Margo's solution is prepared prior to the surgery for direct post-op immersion of 48 hours. The solution consists of 1% formaldehyde and 1.25% glutaraldehyde in 1x phosphate buffer saline.²⁴

Serial dehydration is performed by submerging the sample in ethanol solutions with concentrations at room temperature. For a whole eye sample, the environment is adjusted as followed: for the first three days, dispose 70% ethanol solution and refresh the solution every 24 hours, on the fourth day, increase ethanol concentration to 80% for 8-hour submersion, followed an overnight treatment by 90% ethanol solution. On the last day, use 100% ethanol for three 8-

hour submersion. (In brief, 3×70 % for 24 h, 1×80 % for 8 h, 1×90 % over night, 3×100 % for 8 h) Samples are then kept in dry enclosure afterwards.

To prepare whole eye sample for scanning electron microscopy, whole eye is placed in up-right position and tightly wrapped with aluminum foil and leave the anterior segments exposed. The aluminum foil is placed to increase the sample's conductivity during the SEM. The sample is then taped onto a standard SEM stage with double-sided carbon tapes and sputter coated with Leica AC200 sputter coater, in a rotational deposition mode for a coating thickness of 5 nm.

d. Bacterial Swap culture

Bacterial population at the surface and the surrounding of the implant is investigated through culturing eye swabs before the enucleation of the animal. Sterile cotton swabs are used to collect samples from both eyes of the subject. The swabs are then directly inserted into sterile RPMI culture media and sealed on ice for transport. The culture media is immediately plated onto blood agar plate upon arrival of a certified biological hood.

3.3 Results & Discussion:

Our artificial cornea prototype was successfully implanted into the eyes of two rabbits. The femtosecond laser incision allowed for better initial apposition of epithelium to the implant. However, in both animals, there was a gap between the central optic edge and the cornea that increased over the one-month period. Neovascularization occurred into the gap between implant and lamellar pocket. There were no instances of infection. There were no instances of extrusion. SEM images showed gross preservation of the nanostructures on the central optic. No microbial growth was observed in cultures from either the eye with the implant or control eye.

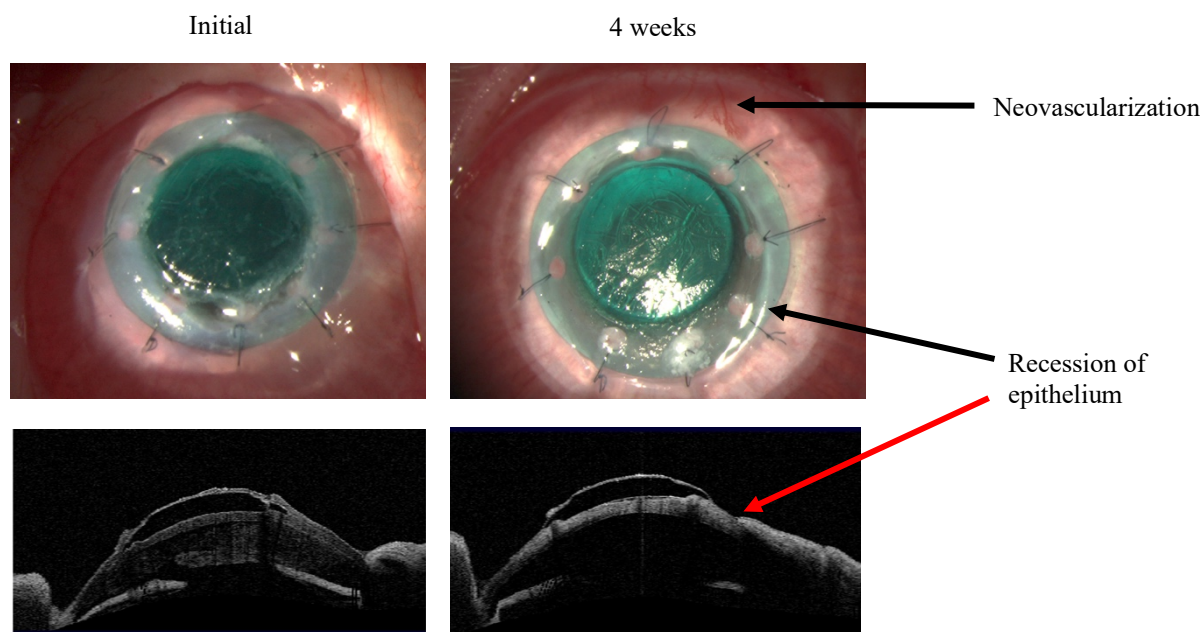


Figure 3.2 Slit Lamp (Top) and AS-OCT (Bottom) of the Implanted Rabbit Eye Before and After One Month Period

Both rabbits survived their one-month implants, under healthy conditions, with no sign of extrusion nor outstanding infections. Although both subjects were in healthy conditions, the study was terminated at early onset. The duration when a normal cornea transplant could be functioning in the eye was traded off for the nanopattern's examination on the device. In situ quality control for nanopatterns is difficult to obtain, and to gather more evidence from a device durability perspective is beneficial at the early development stage. Therefore, in the future studies, the prototypes could potentially be tolerated longer in vivo, paving the way to a more comprehensive and informative cohort.

As shown in the explanted device's micrographs in quality control, the device maintains in good conditions, with nanotopography withstanding the prolonged period of blinking shear. Although some instances of protein deposition on the surface were observed, majority of the surface pertained visible nanostructures. This provides evidence to support the hypothesis that nanotopographic motifs are resilient enough in complex physiological environments, expanding

the possibility of translating this in other challenging conditions such as cardiovascular or pulmonary replacements.

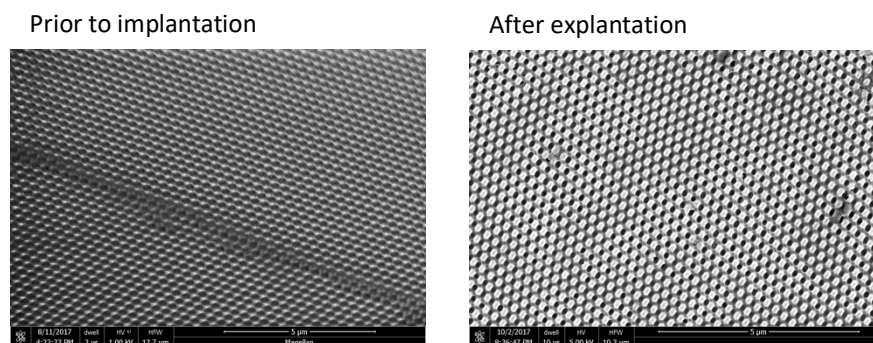


Figure 3.3 Scanning Electron Micrographs Indicates Nanopatterns Retain High Fidelity After One-Month Implant

3.4 Crucial Lessons & Future Directions

The confirmation of the nanotopographic modification could survive and sustain in the harsh environment in the eye, specific address the high shear and frequent eyelid brushing.

The hypothesized long-term protein deposition is also less influential on the surface presence than previously considered. This gives an optimistic outlook for the extending coverage of materials with nanotopography.

The recession of epithelium slowly developed during the pilot trial, which is a sub-optimal clinical outcome. However, the next-step integration of nanoline on the skirt is intended to mitigate the issue. The future trial shall implement the complete nanostructure control to emphasize tissue healing and device integration in animal.

Overall experimental method could be standardized and selectively modified for future use, especially the fixation and in vivo modalities. However, improvement on the bacterial test should be suggested. Gathering more adjacent facility and resources to allow on-site plating and culturing to avoid long distance and freezing cycle would eliminate the false positive of antibacterial effect and provide more insightful data.

Per surgeon's operational feedback, device's flexibility during surgery is desirable. The more elastic and durable polyurethane-based prototype shall be scheduled for ex vivo and possibly in vivo test in the future.

Chapter 4: Fabrication of contact lens for antifungal property with nanotopography

4.1 Motivation

In the upcoming chapters, another ophthalmic product, a bandage contact lens for fungal keratitis, closely spinning off from the development will be detailed. This product's production share similar challenges as previously seen in artificial cornea device, such as the nanopattern transfer onto spherical surfaces. Furthermore, the contact lens manufacturing is proven to have its unique challenges. These challenges underlie in the call for a new hydrogel that not only carries therapeutics, but also advance its effect, but remain mechanically durable and easily manufacturable. Upon preliminary research, chitosan is considered to be a potential candidate that can fulfill all the demands with minor modification or additives. In this following chapter, additives that initiate crosslinking or modify substrates to grant crosslinking ability are discussed.

4.2 Proposed Nanopattern lens fabrication material system: PU/Chitosan

Chitosan is a natural polysaccharide commonly found in shrimp and crab shells. It's a deacetylated derivative of another natural polysaccharide chitin. Chitosan is soluble in strongly acidic environment via the mechanism of protonation of amino side groups. Both chitin and chitosan process good mechanical strength in the dry stage, such as young's modulus and tensile strength. Chitosan also could be processed into a biocompatible hydrogel upon different processing. It has a high glass transition and decomposition temperature and optical transparency.²⁵

Both polyurethane and chitosan exhibit excellent mechanical properties favorable in a commercially viable product. Polyurethane, commercially widely tuned and implemented, offers a huge variety of modulus and processing possibilities, by simply selectively tune the ratio of the synthesized blocks. Polyurethane is resistant to a good collection of common organic solvents, except for DMF, used to process this material primarily here.

Chitosan as a natural biological macromolecule, carries excellent range of mechanical strength adjustable per demand of the application. It's resistant to most organic solvents and soluble in acidic aqueous solution. Unlike other commercial polymers, chitosan's glass transition temperature is comparatively higher.

The mutual exclusivity of the solvent systems used to process polyurethane and chitosan respectively and large different between their glass transition temperatures gives rise to a mean to choose selectively of one of the two in the interfacing combination. The compounded system as a whole is also resilient enough to go through conventional heated and pressurized molding and forming method. Specifically, in our case, when chitosan is cast onto a nanopatterned PU mold and it undergo a lens forming process together, the nanopattern replicated from the casting method onto chitosan will not altered while PU undergo glass transition and adapt the bulk curvature. Afterwards, the PU will be in the lens shape with the nanopatterns protected by the chitosan layer. With either simple peeling or soaking of the double layer in acidic solution, the system could be separated.

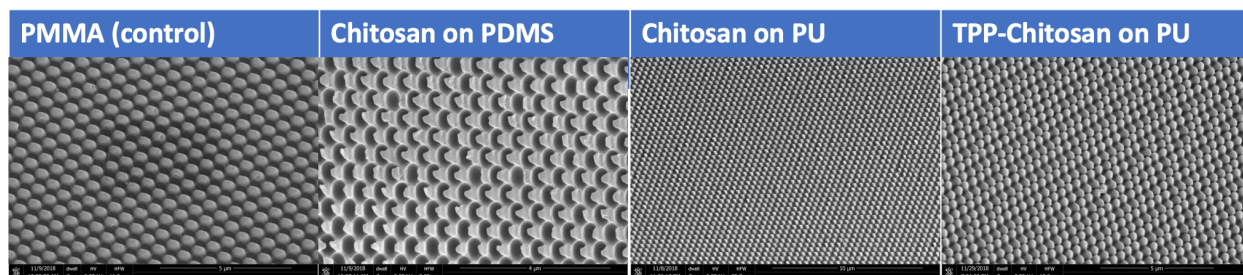


Figure 4.1 SEM of Assorted Chitosan-based Nanopattern and PMMA replica as quality control

4.3 Crosslinking Strategy for Chitosan

4.3.1 Additive Crosslinking as molding strategy: TPP and Glutaldehyde with chitosan

Sodium triphosphate is a commonly used physical crosslinker of chitosan. We tested various concentration (0.1%, 1%, 5% 10% wt) of TPP for producing crosslinked chitosan with nanostructures that withstand substantial swelling in aqueous environment. Currently, using TPP solution of 0.1% wt, 20 mL in volume, to submerge for 30 mins and crosslink patterned chitosan films is the best formula. This product could withstand 48 hours of swelling without the loss of nanotopography. The quantitative height of such surface is still to be determined by AFM, but SEM images suggest non-significant reduction of the structure's height.

Glutaldehyde is a common chemical crosslinker for chitosan, and widely used for biological sample fixation. Similarly to TPP, we tested a range of concentration (0.25%, 0.5%, 2.5%) of Glutaldehyde solution to produce chitosan films with submersion. Although films with nanostructures could be produced, preliminary testing suggests that the structures might not have survived water swelling for over a day. Further evaluation is needed with submersion method.

Glutaldehyde is also attempted to be blended into chitosan solution prior to casting or molding process at various concentration (0.25%, 0.32%, 0.5%, 2.5% wt) to control the set time of the system. In preliminary tests, at or above theoretical critical crosslinking concentration of 0.32%, solutions reach to complete gelation stage with increasing degrees of yellowing.

4.3.2 UV-Crosslinkable N-MAC is a suitable candidate for a bandage contact lens prototype

To further diversity the toolbox of crosslinking and defining the contact lens, the modification of chitosan to grant externally controlled crosslinking activation is explored. N-MAC's is a key adoption driver for contact lens prototype. Previous literatures have various recipes of using different triggers to initiate the crosslinking. The light, specifically UV light activation, is studied with the consideration of future industrial adaptability and

manufacturability. Currently, contact lens manufacturers have broadly utilize pHEMA and silicones in lines of products. Both of these materials' curing process are light-initiated, which has better engineering control for reproducibility and potential for a shorter processing time. If chitosan's derivatives could mirror a majority of those materials, future technological acquisition by existing companies would be smoother with less resistance on their finance and infrastructures.

Among scores of recipes from previous literature, the following modification scheme stands out for the following particular reasons: 1. The modification scheme is short and involves only one chemical, reducing the intensity of advance chemical purification and characterizations. 2. The modification scheme has high specificity and utilize a preferable substitution mechanism, making the yield of the final product higher. 3. The modification involves little highly toxic chemical, addressing the concern of both toxicity of the final product and the currently conscious principle of greener chemistry.

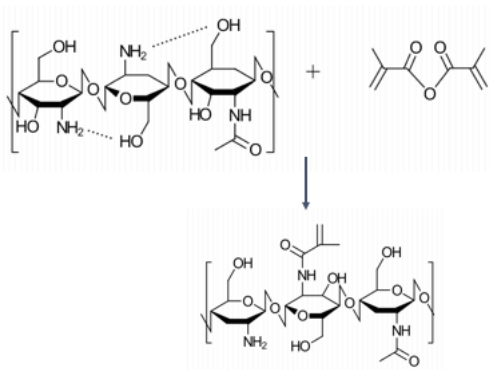


Figure 4.2 N-MAC Synthesis Mechanism: the functional amine group on the deacylated chitosan is attached by one branch of the methacrylate anhydride. The additional substituent carries the double bond required to be UV-activated on demand by radically excited initiators.²⁶

Synthesis:

1% chitosan in 0.1 M acidic acid solution is prepared by gently stirring chitosan powder into the acidic mix for 4-6 hrs at low speed. After the full dissolution, methacrylate anhydride (MA) are added slowly into the solution. The amount of MA is determined by the ratio of anhydride to amino group. The latter used ratio are 4 times of the chitosan's available amino groups, unless specified. The reaction occurs at 60 degree Celsius for 6 hours. The reacted solution will be transferred to dialysis tube with 11-14 k cut-off threshold. The dialysis will be performed against DI water to remove excess MA and acid, for 4 days with replenishment of DI water reservoir every 24 hours. Afterwards, purified solution will be lyophilized for 24 hours to remove all water. The extracts should be snow white sponge-like aggregate. This could reconstitute in neutral purified water overnight.

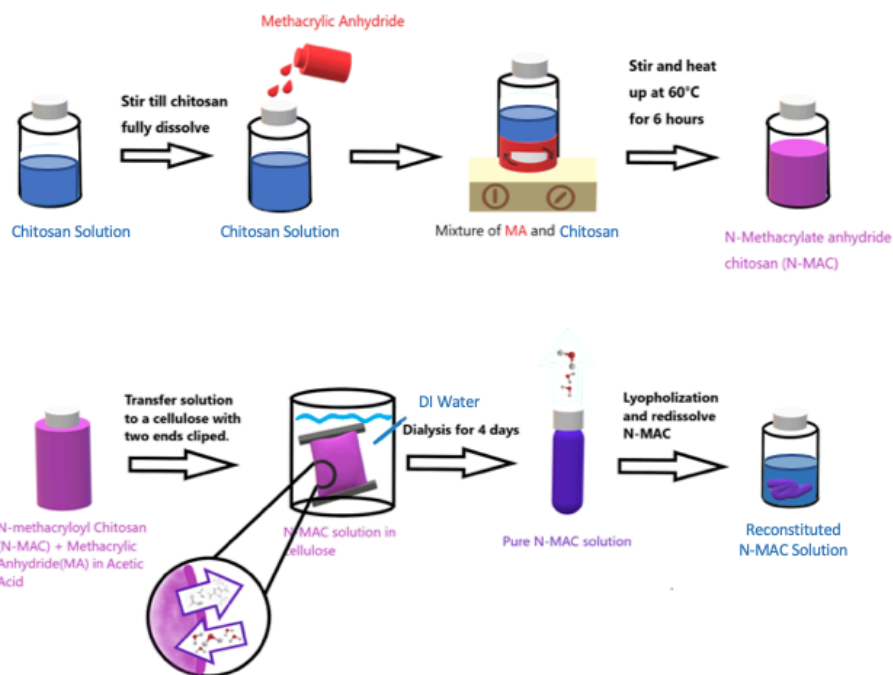


Figure 4.3 Synthetic Workflow Schematics of N-MAC

Material Characterization:

Dried thin film of modified NMAC is characterized using FTIR to locate the modification on the biomolecule. Unmodified chitosan film is used as a control, labeled in black in the figure below. Focusing at the region of 1000-2000 cm^{-1} wavenumber, amide related peaks are accentuated at three specific wavenumbers of 1315, 1536, 1654 (amide $\text{C}=\text{O}$ stretch) cm^{-1} . The additional amides detected in the spectrum represent the successful modification of the chitosan's amine group with methacrylic group, enabling the molecule's photocrosslinking capability. Within the 1000-1800 range, a few other peaks that are potentially representing Alkenyl $\text{C}=\text{C}$ Stretch (1680-1620 cm^{-1}) also more substantial in the modified NMAC than the regular chitosan. Furthermore, to confirm that our purification process is effective, no $\text{C}=\text{O}$ anhydride bonds is detected in the adjacency of 1800 cm^{-1} , representing the exclusion of methacrylic anhydride (MA)'s presence in the film.

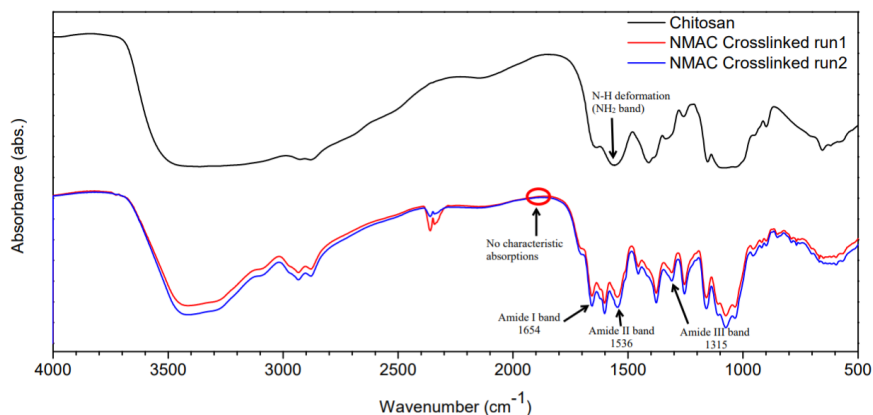


Figure 4.4 FTIR Spectrum of N-MAC showing the addition and alteration of amine group and double bonds

Swelling Behavior:

UV-crosslinked N-MAC hydrogel is also evaluated for its swelling and drying behavior with water to gauge the impact of the physiological environment on the release of potential therapeutic payloads based on its fabrication exposure process.

The hydrogel is crosslinked with a deposit of 80 μL of 1wt% N-MAC solution in MilliQ water on a mold of a PDMS artificial cornea mold for different duration (5/15/30 mins), at the 50% relative maximum exposure power. The swelling sample is submerged MilliQ water in a closed well plate and the drying sample is left in opened well plate to air dry. The weight of the samples is measured hourly for short-term study and every 8 hours for 24 hours in long term group.

The figure below shows the sample's relative change of water content in percentage. Among three different exposing protocol, all N-MAC exhibits maximum water intake in approximately the same period of around 1.5 hours and start to reduce weight in a consistent manner, while drying rate reaches plateau differently but yield the same remnant mass. The 15 mins crosslinking exposure show distinguishing behaviors while experiencing gaining and losing water in the hydrogel. The 15-min hydrogel intake significantly 40% less water contents than the other two exposure length. Its drying pattern reaches the deflecting point of 2.2 hours, earlier than 5- and 30-min samples. These two trends suggest that an optimal time point exists around 15 mins for minimal water intake.

Under a given modification ratio, there will be a sufficient amount of radiation that could result in the vast majority of the crosslinkable $\text{C}=\text{C}$ double bonds to be thoroughly reacted. Lack of exposure could leave some of the viable sites unused that forms a looser material network that enable more expansion and water infiltration. Overexposure of strong UV radiation, on the other

hand, may have introduced cleavage of polymeric chains that reduce network connectivity, leading to high swelling ratio.

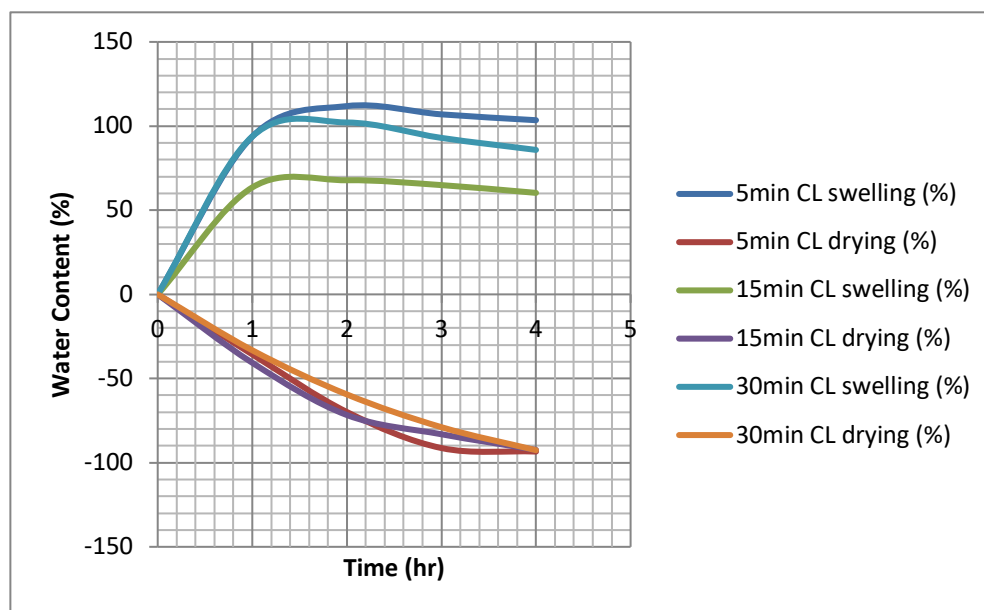


Figure 4.5 Consistent Swelling and Drying Behavior of N-MAC under Various Crosslinking Exposure Time

The figure below shows the light absorption of chitosan and derivative products across the 300-750 nm spectrum, covering the 400-700 nm visible light range. Samples measured are prepared by dispensing 10 μ L of each type of sample into a well on 96-well plate for standardized UV-Vis measurement. The volume and the thickness used for measurement is consistent with the murine lens fabrication. Within the visible spectrum, all samples, either modified or non-modified chitosan sample, record less than 4% absorption of light, considered to be exceptionally above the standard requirement in the contact lens industry, where acceptable commercial lens products generally record less than 10% loss from the light source.

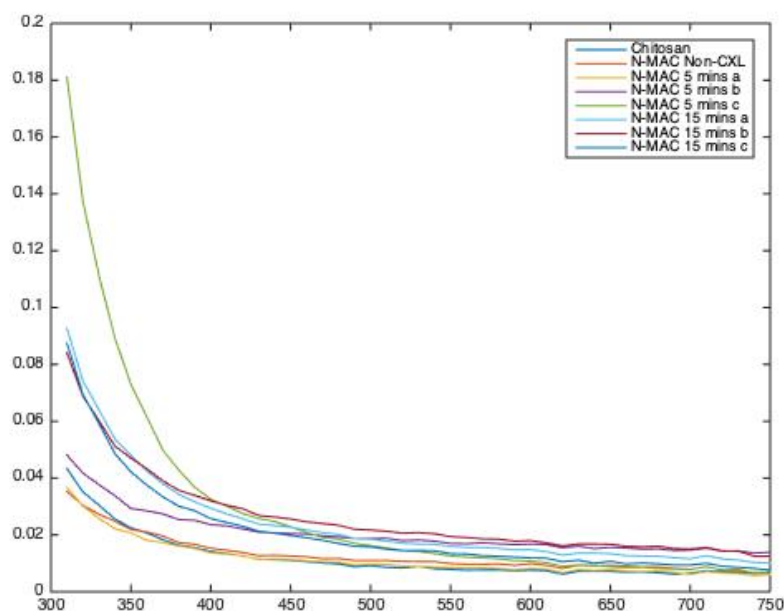


Figure 4.6 UV-Vis Absorption Spectrum of the Crosslinked N-MAC Shows Minimal Absorption of Visible Lights

N-MAC possess more capability as a nanopattern carrier material than commercial pHEMA. In the rise of the question where some hydrogels, such as pHEMA, present high surface tension during swelling process that could smoothen and erase the implemented nanopatterns, the new N-MAC needs to be tested for its capability to retain nanotopographic surface modification during potential swelling during fabrication and storage of the lens production.

N-MAC hydrogel Crosslinking Protocol:

In brief, 10 μ L of 1wt% N-MAC solution is pipetted onto the P500 polyurethane mold and cured for 5-10 mins until gelation. The hydrogel is fixed a serially dehydrated with 2.5% glutaraldehyde and 50-100% ethanol solution. The gel is then detached and prepared for SEM.

Following crosslinking protocol, fixing and dehydration process, a N-MAC film is nanopatterned via a PU nanopattern mold and imaged in dry condition under SEM. The P500 nanopatterns are replicated faithfully and retained at the surface of the hydrogel, shown in the representative SEM image below.

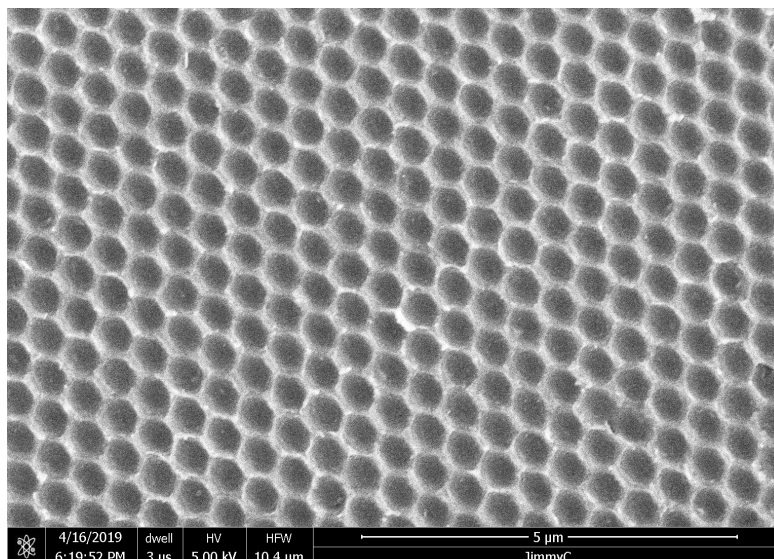


Figure 4.7 Nanopatterned N-MAC Gel Surface Has Good Fidelity of the Reverse Replication

The presented SEM has shown reverse replication of the nanopattern of p500 pillars in good fidelity, where the close-packed configuration and the periodicity are closely resembling its master. The height of the pillars is less consistently measured by AFM, possible for the nature low elastic modulus of the hydrogel. This sample is also measured after dehydration process to accommodate the high vacuum environment for SEM operation. It's possible that some of the crosslinking effect taken place in the same is contributed by the post processing fixative, rather than modified hydrogel's photo-initiated crosslinking alone. This hypothesis could be validated in the future with the availability of an environmental SEM at lower vacuum level or a liquid AFM that scans humidified samples. Despite the limitation of characterization technique, this sample provide insights that the photocrosslinking chitosan could be more enduring as a nanopattern carrier than commercially prevalent pHEMA, which is essential to materialize the proposed integration of nanopatterns on a softer class of polymeric material.

4.4 Conclusion:

The results prove that biocompatibility and toxicity shall be included and even prioritize in the consideration of modification of biomaterials, such as N-MAC, that will be implemented into clinical application. Moreover, the functional demands such as mechanical constraints, dimensions, fabrication endurance, and specifically in this instance, the optical clarity and coloring, is vital for a clinically translatable product.

Chapter 5 Mouse and Rabbit model for antifungal efficacy test

5.1 Motivation

Although rodent models are popular *in vivo* platform to in the study of ophthalmology, researcher has limited access to customized murine fitted contact lens at a high cost. Researcher currently deploy strategies such as performing eyelid closure surgery or settle for equivalent *in vitro* cell culture models instead. Such compromises made for the lack of easy access to convenient better fitted manufacturing scheme are hindersome to produce relevant results for ocular pharmaceutical products. The technical challenge of fabricating murine lens rooted at the steep curvature of the natural mouse eye. Previous literature provided example measurements of 6 weeks old C57BL/6 mice indicated a corneal diameter of 3.2 mm and SAG (Sagittal Depth) of 1.5 mm and lens thickness are generally ~20% of its average diameter (0.6 mm).¹⁸ Although previous works occasionally show the possibility of making fitted lens in lab, such lens currently requires specialty machines and skilled technicians to produce, limiting the quantity and access to the scientific community at large. For more reproducible and statistically analyzable data set, a scalable and widely distributable method is essential to advance eyecare solutions.

In this chapter, a simple, and scalable molding method to produce murine fitted contact lens is discussed. The recipe tackles the challenging dimension problem with popular lab supplies at an affordable price range, in hope of expanding researchers' capability to arrange larger animal cohort in the future.

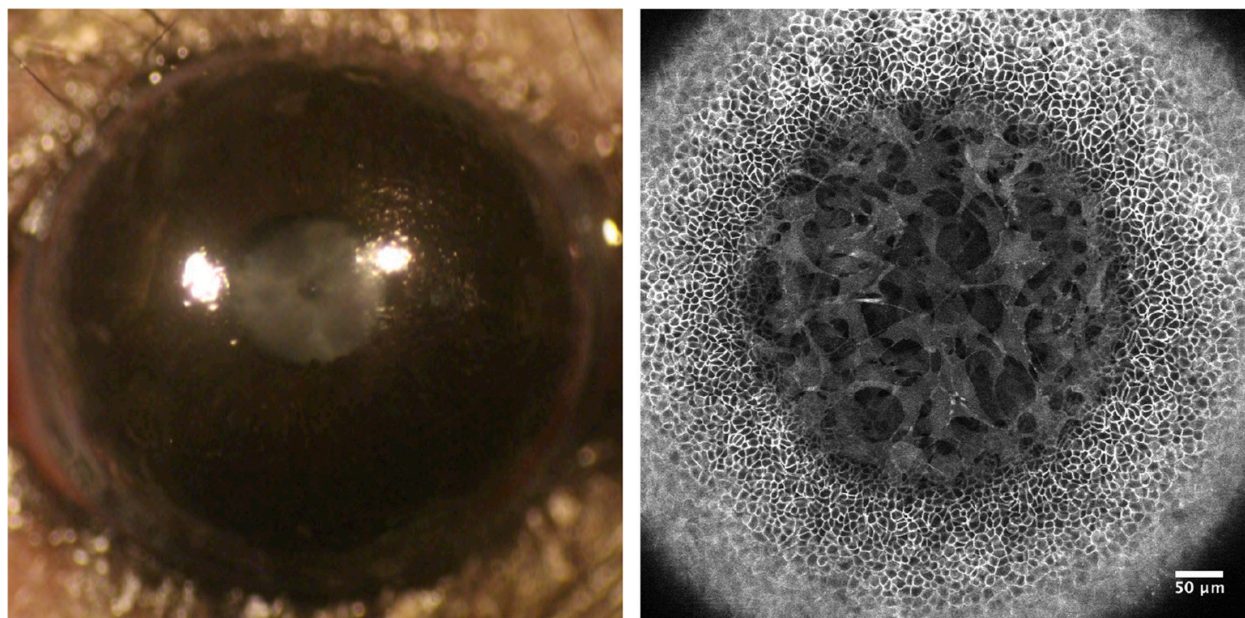


*Figure 5.1 Representative images of a murine cornea after wearing a *P. aeruginosa*-inoculated CL for 22 days without the development of bacterial keratitis. Dissection microscope image (left) and confocal image (right) ¹⁸*

5.2 Murine Model Contact Lens Fabrication Protocol

Murine fitted lens mold is molded following the procedure illustrated below. 3mm glass beads coated with Teflon or other anti-adhesives are used as the model of a murine eye. A thin supportive layer (1-1.5 g) of PDMS is first cured at the bottom of a detachable cup. After 2 hours of solidification, a thin spread (~0.5 g) of PDMS is added on top of the cured layer. Glass beads is then carefully placed in the container and the mold is baked again for 2 hours at 110 C. After curing, the glass beads are twisted and discarded.

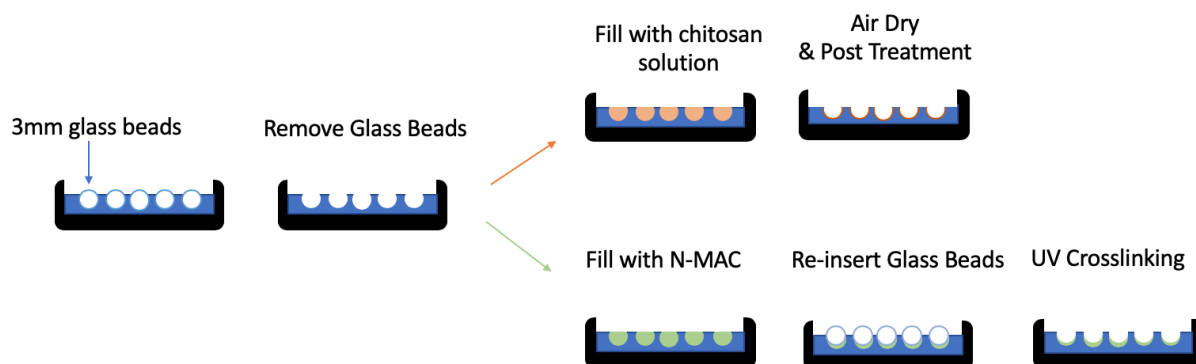


Figure 5.2 Fabrication of murine lens mold and molding mouse lens with two chitosan-based hydrogels

For a 3-mm diameter chitosan-TPP lens, 10-15 μL of the 2% chitosan solution is pipetted in a lens mold, and air dried at room temperature for 4 hours. The lens is carefully lifted and detached from the mold. The lens is crosslinked by 10wt% NaOH for 1 minute and followed by 0.1wt% TPP solution for 5 minutes. The crosslinked lens is then submerged into PBS for storage at room temperature.

For gelation of a 3-mm diameter lens, 5 or 10 μL of the 1% N-MAC photocrosslinkable chitosan solution is pipetted in a lens mold, and a 3-mm glass bead is placed onto the drop. The assembly is exposed to UV lamp at its 50% relative intensity, 5 mm away from the leading probe tip. The lens is carefully lifted and detached from the mold and the bead and submerged into PBS for storage at room temperature. Figure D-JC demonstrate the product's clear and highly spherical resemblance to a murine contact lens.

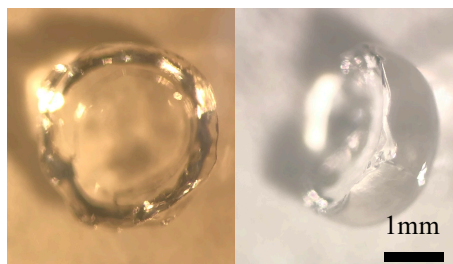


Figure 5.3 Murine lens of N-MAC under stereomicroscope, bottom-up view (left) and side view (right)

5.3 Lens In Vivo Fitting Results

Previously described mouse fitted lens are tested for the mouse's wearing comfort and compliances. The fabricated prototypes are sterilized with UV lamp in biohood and/or extensively washed with sterile PBS solution before animal use. The lens is fitted to the anesthetized mice with surgical tweezers under optical microscope. Mice are left to recover and resume normal activity after operation. Images of the mouse eyes wearing the Chitosan-TPP contact lens are shown at two different focal point. The lenses adhere well with only one single lens falling out of 5 pairs lens tested after 1 day.

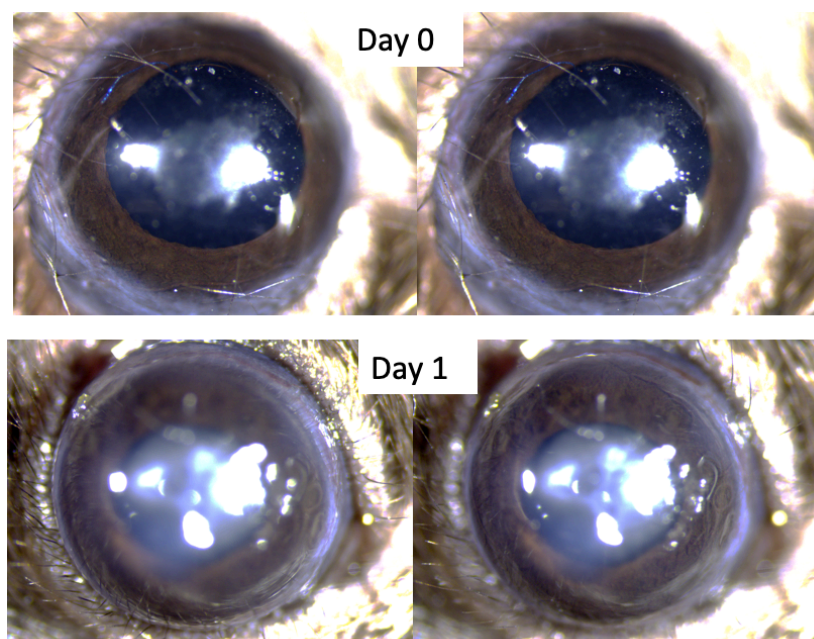


Figure 5.4 Murine lens of Chitosan-TPP fitted under microscope, initial time point view (top) and after one day (right)

5.4 Further Work

To investigate further about the fitness of the lens on the cornea, Anterior segmented optical coherent tomography could be used to visualize the cross-sectional profile of the nearby of the cornea. AS-OCT is more prevalent for larger animal model such as rabbits and human while murine specific AS-OCT is not widely commercially available but potential academic

contacts within centralized ophthalmological research institute could provide adapting guidance. Live Fluorescent microscopy similar Matteo et al. used above would also be informative to visualize underlying tissue's recovery and potentially the fungal activity in tandem. Future monitoring of the mouse behavior will be improved by adding in-cage surveillance camera for continuous discomfort monitoring and timely response to other urgent situation possibly caused by infections.

5.5 Potential vessel for constructing a Fungal Infection Induction Model

The mouse fitting contact lens could not only realize the sustain delivery of the drug for the proposed therapeutic standpoint, but also could be applied for a pathology study angle where the pathogen contaminated lens appears in daily use could be quantitatively mimicked. A brief illustration below demonstrates the application of the proposal. This proposed model would be advantageous for studying what is the public health implication of the popular non-sterile consumer habit.

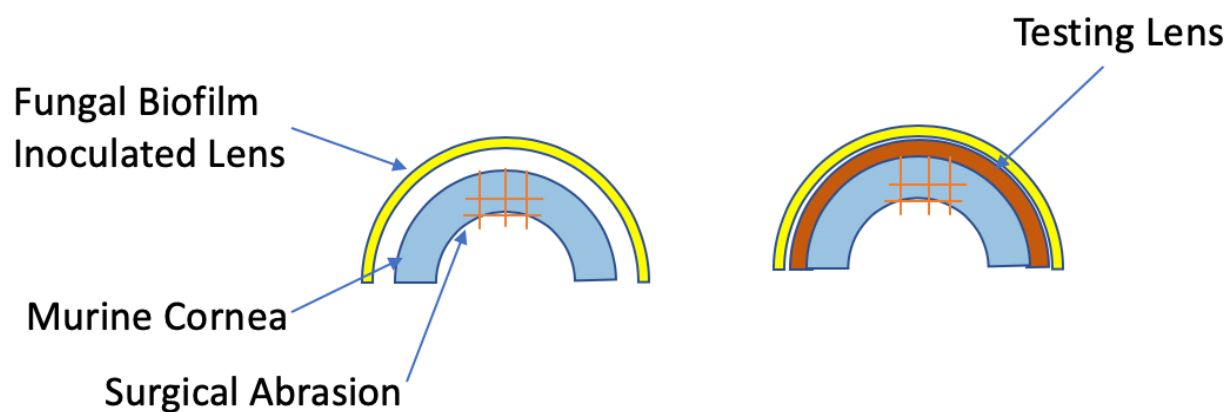


Figure 5.5 Illustration to Apply Fungal Infection Induction Model

Chapter 6: Vacuum Assembly for Tunable Lens Fabrication

6.1 Motivation

Tunable and larger lens for other model's fitted lens fabrication such as rabbits would be demanded in the near future to advance preclinical validation. To adjust to the model's dimension appropriately, machinery for variable and reliable fabrication is needed. In this half of the chapter, an assembly is sketched out to incorporate those in lab production needs, primarily on achieving the proper curvature.

6.2 Materials and Method

The system is enabled by the previously mentioned polyurethane (PU) nanopattern mold. (chapter 2) The flexible nature of the thin PU mold could conform onto the supportive assembly structure under uniform pressure application. Such pressure is delivered by using vacuuming. Negative air pressure could avoid local and concentrated solid contacts that damage nanopattern molds. The uniformity of air pressure is also desirable to prevent the thin mold folds or wrinkles instead of expansively conforms onto molds. Smooth finishing is crucial for contact lenses for both wearing comforts and optical clarity.

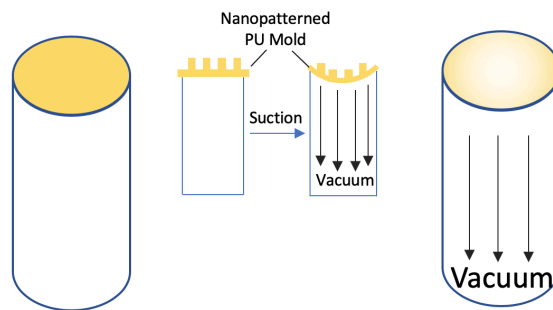


Figure 6.1 Mechanistic Illustration of Vacuum Lens Fabrication Assembly

The assembly comes in two parts, inspired by the previous work used for reversal imprinting.²¹ The top plunger is designed to secure the mold's position with the alignment pins and seal off air leakage from the thin film's fringes. The cover could also avoid particle falling off during productions, should it occur. The dome-shaped base contains the customizable spherical supportive structure visible from the top-down view, centered in the 22x22 mm squared slot that tightly fit the thin PU mold cast from standard nanopattern masters. A small through hole connecting from the bottom of the lens to the bottom of the assembly, allowing negative air pressure to convey through. The ring surrounding the hole for easy insertion for tubing.

The assembly is intended to be 3D printed and polished with metals such as aluminum, steels or coppers. The 3D printing method, especially for the dome-shaped base, is convenient to switch the supporting curvature, accordingly to clinical measurement such as OCT, without major change in the prototyping method. The material choice is to provide a mechanically sound and heat-conductive environment. Minor heat could expedite the evaporation in drop casting processing, allowing faster turnaround time in larger experimental group.

6.3 Parts and Expose-Cut Assembly

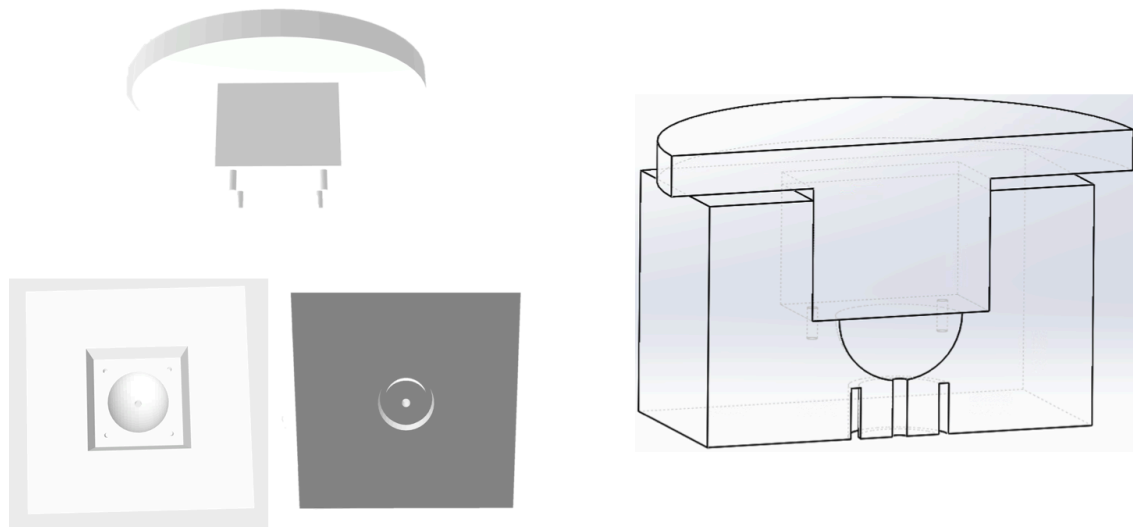


Figure 6.2 Solidworks Rendering of Vacuum Lens Fabrication Assembly (Left: by parts; Right: by Closed Assembly)

6.4 Generic Protocol for Lens Prototyping with Vacuum Assembly

Part 1: Fabrication of PU nanopattern mold

1. Dropcast 10wt% 72D in DMF solution on the nickel mold
2. Dry on hot plate around 70 °C
3. Without peeling of the PU film, transfer to tetrahedron, use two Teflon film for sandwiching
4. Imprint protocol:
 - a. 266°F, 1.0 klbf, 5 mins
 - b. 88°F, 1.0 klbs, 5 mins
5. Remove Film from mold as negative mold

Part 2: Assembly in vacuum mold

1. Insert PU negative mold film into the mold hole of the base assembly, pin down by alignment pins

2. Stabilize the assembly and insert the vacuum tubing in the bottom, turn on suction and smoothen out the mold in the spherical dimple gently
3. Dropcast desired solution (eg. Chitosan) onto the nanopatterned mold and air dry for lens prototype (generally takes 2-3 hrs)
4. After drying, carefully use tweezers to detach the lens from the PU nanopattern mold

Chapter 7: Commercialization Exploration of Artificial Cornea and Contact Lens

7.1 I-CORP Experimental Iteration

7.1.1 Motivation

The customer discovery phase on the entrepreneurial market research intends to survey a wide range of industrial stakeholders' opinion and sentiments. Eventually the project improves the presentative message of our product.

7.1.2 Research Method

Weekly, 10 interviews of 10-15 mins with directly involved personnel are arranged. Participants include ophthalmologist, corneal specialist, registered nurses, eye-care corporate marketeers, academic professors, and venture capitalists and patent attorneys. Questionnaires are curated customarily. Note and transcriptions are prepared afterwards for analysis. Project pitch is edited at the end of each week after integrating useful input from fellow project trainees and interviewees. Four iterations, 42 participants are recruited during the one-month refining period.

7.1.3 Results

Table 2: Value Proposition Progression

1 st Proposition	The NanoCurv is an artificial cornea marketed for ophthalmologists located at hospitals and eye care centers in the US that will decrease postoperative complications and eliminate patient reliance on eyedrops.
Revision Comment	For statement clarity for pitching, suggested to consolidate the initial proposition and reduce use of medical jargons.
2 nd Proposition	Our corneal replacement restores patients' sight for longer than a donor cornea by reducing the likelihood of complications and rejection.
Revision Comment	Narrow down more responsive key features.
3 rd Proposition	NanoCurv is an artificial cornea that could help patients recover faster by decreasing the rejection rate, providing more customized vision and reduce long term steroidal drop use. For medical device companies, the device has longer shelf life and easier storage at a lower cost.
Revision Comment	Research further towards relating indications/medical issue onto part(s) of the product's value proposition
4 th Proposition	NanoCurv is an artificial cornea that could help patients recover faster by decreasing the rejection and infection rate, providing more customized visual outcome and reduce long term steroidal drop use. For medical device companies, the device has longer shelf life and easier storage at a lower cost. Especially in urgent cases such as warzones and chemical attack, the device provides instant accessibility under insurgence.

Table 3: Target Customers

1 st Proposition	Ophthalmologists/Eye Care Center Admin/Hospital Admin
Revision Comment	The popular surgical occurring sites are eye clinics and dedicated ophthalmic institutes instead of general hospitals. Suggested to remove Hospital admin from the list for specificity.
2 nd Proposition	Ophthalmologists/Eye Care Center Admin
Revision Comment	Be more specific and tailor values onto targeted customer segments
3 rd Proposition	U.S. ophthalmologist and patients relevant to full thickness replacement, and corresponding eye care centers admins for logistics.
Revision Comment	Further define customers in more marketable details.
4 th Proposition	U.S. Ophthalmologist/US full thickness replacement patients with previous graft failure or keratoconus. For institutions, high volume U.S. Eye centers are primary targets.

7.1.4 Discussion and Future Work

Customer discovery process is greatly beneficial to both the product as well as the development team to understand the medical, societal and financial problem an artificial cornea device is addressing. We recognize that our domestic needs are relatively niche and mature while overseas demands are more attractive financially and logistically complex at the moment. For the project development at current stage, the team and future potential cooperation entity would be advice to approach domestic partnerships for funding, and dedicated networks of distribution to gain overseas interests and negotiate international partnerships with the established templates used in the United States.

With the latest waves of interests to encourage biomedical entrepreneurship, a collection of competitions and initiatives are available for not only seed funding, but also connection to venture capitalists and wider range of medical professionals in the field.

7.2 New Venture Competition (NVC)

In continuum of the effort to explore the commercial viability of the NanoCurv artificial cornea, the New Venture Competition (NVC) is served as a suitable testing ground prior to the product's official move into its corporation goal. Not only does NVC introduces universally accepted formats to formulate a future pitch for products and company development, but also acts as a platform to connect both local and international partners to us via showcasing. The competition's success will entitle the project with small amount of financial support and publicity in the ophthalmic field for further attracts institutional support and capitals.

The participating in the competition yields two primary deliverables: 1. The concept paper, a short booklet with rich but summative illustrative facts and analysis to draw in initial interests of investors and judges. 2. The pitch desk, a 12-minute scripted presentation for more

detailed pitching events to advance our product’s story and imagery and cover logistics details to ground investors into negotiation track.

In the process of producing aforementioned product, both academic and business research are advances. Particularly, in terms of business research, market analysis, competitors, and business models are crucial segments to cover in both documents. A few essential takeaways are below:

1. For the U.S. domestic niche market for cornea transplant has relatively maturity and self-sustainability, global presence and international partnership would be crucial to reach to patients in needs.
2. However, direct sales with global presence across continentals requires large amount of capital and long period for customers and regulatory relations. Drafting partnership agreement with well-established eyecare corporate such as Alcon and CorneaGen could fast track product distribution and approvals.
3. Conservatively, to roll out the proposed model, roughly \$5 million will need to be raised in the first 2 years to cover R&D expenses and partnership legal proceedings, until the first sales of products.



Figure 7.1. Schematics of revenue streams in the proposed licensing business model for global expansion.

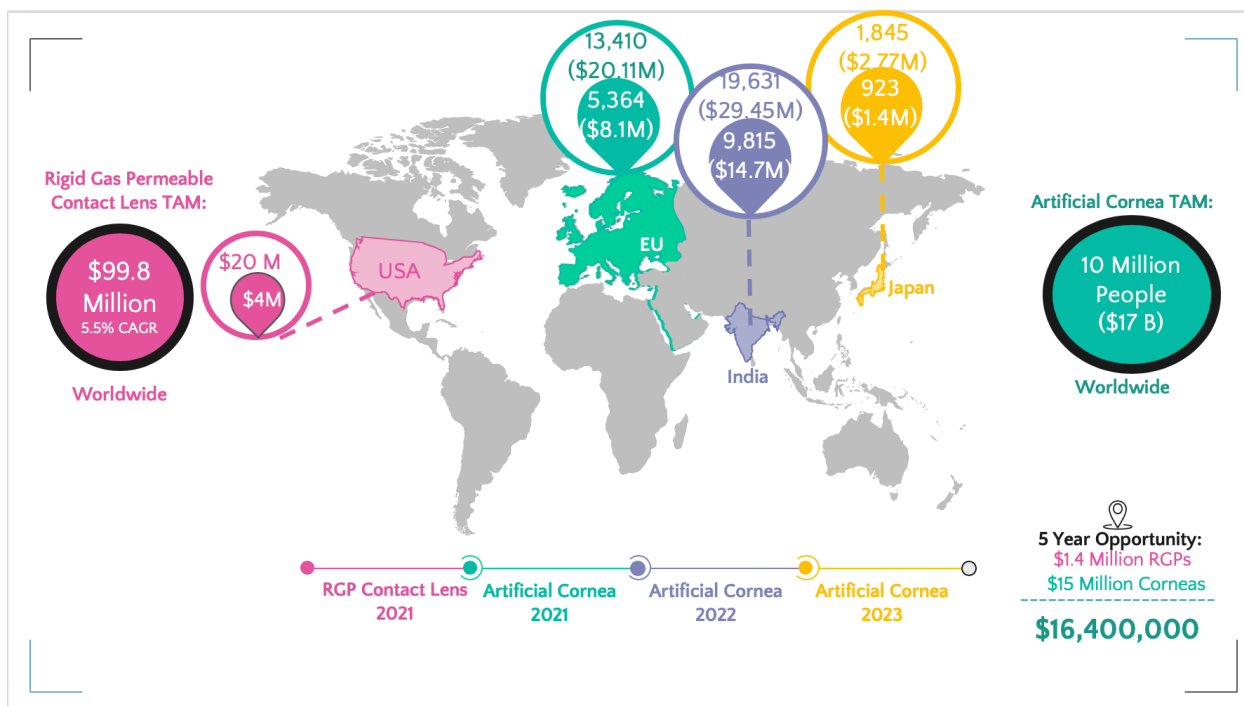


Figure 7.2 Total available market (TAM, in large circles) and Serviceable Obtainable Market (SOM, in raindrops) of potential regions around the globe. Projected business advancement timeline is also listed below in maps. With licensing model, the combine of both product line internationally could generate an estimate revenue of \$16.4 M. Credit: Wyobroski and Cai

Chapter 8. Future Outlooks

Looking ahead, medical solutions for corneal disease have a bright future. Besides propelling further with validating and commercializing efforts for our ophthalmic projects, we should also stay updated and connected with other researchers in the field. Representatives in four categories are covered for future references and possible collaborative talk.

1. From the aspect of using wound healing promoting biomaterials, Massachusetts Eye and Eye Infirmary's researcher Dr. Dana Reza utilizes similar decoration scheme as the N-MAC modification mentioned in Chapter 4, on gelatin, another popular biomaterial. Chitosan could potentially have additional antimicrobial effect, compared to the gelatin derivative GelCore, but lacks the easy processing gelatin molecules are.²⁷

2. Taking advantages of a complete acellular material approach, recent attentions were drawn to Gore-Tex by W.L. Gore, a long time Teflon experienced cooperation by Bloomberg. Although short of academic publication, the disclosed timeline for the company is comparable to our project's stage. Teflon has been the platform for many medical application for its strong non-adhesive surface property. Nanopattern as a versatile tool to tune surface property, could possibly applied in more materials than ones covered in the limited thesis.²⁸
3. From a regenerative medicine perspective, Dr. Nishida's lab has strengthened corneal stem cell's understanding.²⁹ More stable differentiation methods on corneal stem cells could provide the cellular components our product is trying to better interface with. Furthermore, Dr. Evelyn Yim's lab paths on specifically useful insights of nanopatterns and stem cell.³⁰

In sum, with our unique expertise, extending our materials and fabrication methods as a platform and reach over to cellular and molecular control to create the comprehensive treatment option would be promising.

References

- (1) Costanzo, Linda S.. Physiology,, Elsevier, 2013. ProQuest Ebook Central, <http://ebookcentral.proquest.com/lib/uci/detail.action?docID=1479991>.
- (2) Facts About the Cornea and Corneal Disease | National Eye Institute. <https://nei.nih.gov/health/cornealdisease>
- (3) Optical Properties of the Eye - American Academy of Ophthalmology. <https://www.aao.org/munnerlyn-laser-surgery-center/optical-properties-of-eye>.
- (4) Nowell, C.; Radtke, F. Corneal Epithelial Stem Cells And Their Niche At A Glance. *Journal of Cell Science* 2017, jcs.198119.
- (5) Optical properties | Technology by Covestro. <https://www.tpu.covestro.com/en/Technologies/Properties/Optical-Properties>.
- (6) Lewandowska, K. PHYSICO-CHEMICAL PROPERTIES OF CHITOSAN COMPOSITES WITH SYNTHETIC POLYMERS AND INORGANIC ADDITIVES. *Progress on Chemistry and application of Chitin and its Derivatives* 2015, XX, 162-169.
- (7) Deep Anterior Lamellar Keratoplasty (DALK) - Ophthalmic Consultants of Vermont. <https://ocvermont.com/corneal-surgery/deep-anterior-lamellar-keratoplasty-dalk/>.
- (8) 2017 EYE BANKING STATISTICAL REPORT; Eye Bank Association of America: Washington, DC, 2017.
- (9) Rein, D. The Economic Burden Of Major Adult Visual Disorders In The United States. *Archives of Ophthalmology* 2006, 124 (12), 1754.
- (10) Bourne, R. Magnitude, Temporal Trends, And Projections Of The Global Prevalence Of Blindness And Distance And Near Vision Impairment: A Systematic Review And Meta-Analysis. *Lancet* 2017, 5.
- (11) Chakravarthy, U.; Biundo, E.; Saka, R.; Fasser, C.; Bourne, R.; Little, J. The Economic Impact Of Blindness In Europe. *Ophthalmic Epidemiology* 2017, 24 (4), 239-247.
- (12) Economic Studies|Vision Health Initiative (VHI)|cdc.gov. https://www.cdc.gov/visionhealth/projects/economic_studies.htm.
- (13) Hammersmith, K. National Outbreak Of Acanthamoeba Keratitis Associated With Use Of A Contact Lens Solution, United States. *Yearbook of Ophthalmology* 2010, 2010, 117-118.
- (14) Dart, J.; Radford, C.; Minassian, D.; Verma, S.; Stapleton, F. Risk Factors For Microbial Keratitis With Contemporary Contact Lenses. *Ophthalmology* 2008, 115 (10), 1647-1654.e3.
- (15) Collier SA, Gronostaj MP, MacGurn AK, Cope JR, Awsumb KL, Yoder JS, Beach MJ. Estimated burden of keratitis — United States, 2010. *MMWR Morb Mortal Wkly Rep*. 2014;63(45):1027-30.

- (16) Dickson, M. (2017). Towards a Scalable, Biomimetic, Antibacterial Coating. UC Irvine. ProQuest ID: Dickson_uci_0030D_14370. Merritt ID: ark:/13030/m5895zk2. Retrieved from <https://escholarship.org/uc/item/4br3n017>
- (17) Ivanova EP, Hasan J, Webb HK, et al. Natural bactericidal surfaces: mechanical rupture of *Pseudomonas aeruginosa* cells by cicada wings. *Small*. 2012;8(16):2489-94.
- (18) Dickson MN, Liang EI, Rodriguez LA, Vollereaux N, Yee AF. Nanopatterned polymer surfaces with bactericidal properties. *Biointerphases*. 2015;10(2):021010.
- (19) Rosenzweig, R.; Perinbam, K.; Ly, V.; Ahrar, S.; Siryaporn, A.; Yee, A. Nanopillared Surfaces Disrupt *Pseudomonas Aeruginosa* Mechanoresponsive Upstream Motility. *ACS Applied Materials & Interfaces* 2019, 11 (11), 10532-10539.
- (20) Teixeira AI, Abrams GA, Bertics PJ, Murphy CJ, Nealey PF. Epithelial contact guidance on well-defined micro- and nanostructured substrates. *J Cell Sci*. 2003;116(Pt 10):1881-92.
- (21) Dickson, M.; Tsao, J.; Liang, E.; Navarro, N.; Patel, Y.; Yee, A. Conformal Reversal Imprint Lithography For Polymer Nanostructuring Over Large Curved Geometries. *Journal of Vacuum Science & Technology B, Nanotechnology and Microelectronics: Materials, Processing, Measurement, and Phenomena* 2017, 35 (2), 021602.
- (22) Gauss, C. F. (2005). Pesic, Peter (ed.). *General Investigations of Curved Surfaces* (Paperback ed.). Dover Publications. ISBN 0-486-44645-X.
- (23) Kakisis, J.; Antonopoulos, C.; Mantas, G.; Alexiou, E.; Katseni, K.; Sfyroeras, G.; Moulakakis, K.; Geroulakos, G. Safety And Efficacy Of Polyurethane Vascular Grafts For Early Hemodialysis Access. *Journal of Vascular Surgery* 2017, 66 (6), 1792-1797.
- (24) Margo, C.; Lee, A. Fixation Of Whole Eyes: The Role Of Fixative Osmolarity In The Production Of Tissue Artifact. *Graefe's Archive for Clinical and Experimental Ophthalmology* 1995, 233 (6), 366-370.
- (25) Zargar, V.; Asghari, M.; Dashti, A. A Review On Chitin And Chitosan Polymers: Structure, Chemistry, Solubility, Derivatives, And Applications. *ChemBioEng Reviews* 2015, 2 (3), 204-226.
- (26) Li, B.; Wang, L.; Xu, F.; Gang, X.; Demirci, U.; Wei, D.; Li, Y.; Feng, Y.; Jia, D.; Zhou, Y. Hydrosoluble, UV-Crosslinkable And Injectable Chitosan For Patterned Cell-Laden Microgel And Rapid Transdermal Curing Hydrogel In Vivo. *Acta Biomaterialia* 2015, 22, 59-69.
- (27) Shirzaei Sani, E.; Kheirkhah, A.; Rana, D.; Sun, Z.; Foulsham, W.; Sheikhi, A.; Khademhosseini, A.; Dana, R.; Annabi, N. Sutureless Repair Of Corneal Injuries Using Naturally Derived Bioadhesive Hydrogels. *Science Advances* 2019, 5 (3), eaav1281.
- (28) Bennett, D. Bloomberg Businessweek. 2019.

- (29) Hayashi, R.; Ishikawa, Y.; Sasamoto, Y.; Katori, R.; Nomura, N.; Ichikawa, T.; Araki, S.; Soma, T.; Kawasaki, S.; Sekiguchi, K.; Quantock, A.; Tsujikawa, M.; Nishida, K. Co-Ordinated Ocular Development From Human Ips Cells And Recovery Of Corneal Function. *Nature* 2016, 531(7594), 376-380.
- (30) Rizwan, M.; Peh, G.; Adnan, K.; Naso, S.; Mendez, A.; Mehta, J.; Yim, E. Cell Therapy: In Vitro Topographical Model Of Fuchs Dystrophy For Evaluation Of Corneal Endothelial Cell Monolayer Formation (*Adv. Healthcare Mater.* 22/2016). *Advanced Healthcare Materials* 2016, 5(22), 2960-2960.